




# Energy-Spectral-Efficient Heterogeneous Cellular Networks: Joint Optimization of Cross-Tier Inter-BS Cooperation and BS Deployment

Guogang Zhao , Sheng Chen , *Life Fellow, IEEE*, and Lajos Hanzo , *Life Fellow, IEEE*

**Abstract**—This paper enhances the energy/spectral utilization of a large-scale coordinated multi-point (CoMP) enabled two-tier heterogeneous cellular network (HCN) by the joint optimization of the associated cross-tier inter-BS cooperation and BS deployment, where a pair of BSs in different tiers can cooperate to transmit desired signals to the user equipment (UE) supported. We derive the energy-spectral efficiency (ESE) for the large-scale CoMP-enhanced two-tier HCN. Our ESE modeling distinctively includes: 1) The ESE's dependence on the activation degree of cross-tier inter-BS cooperation is quantified, which can be flexibly harnessed for transforming the grave interference-limited situation of the tier-edge UEs into harmonious CoMP-support. 2) Both the BS densities in these two tiers and the large-scale user-behaviors (LSUBs) are explicitly integrated into our ESE modeling. Under this tractable ESE model, we first optimize the network's ESE by choosing a suitable cooperation activation degree based on a specific cellular scenario, whilst satisfying the UE's outage constraint. We continue by formulating the joint optimization problem of the cooperation activation degree and of the BS density for maximizing the ESE, while varying the LSUBs. Our simulation results confirm the accuracy of our ESE modeling and quantify the impact of network parameters on the achievable ESE. We demonstrate that the proposed joint optimization strategy has a significantly higher ESE than its optimization counterpart only considering the cooperation activation degree. Our solution may be expected to pave the way for improving the resource efficiency of large-scale dense HCNs.

**Index Terms**—Large-scale dense cellular networks, energy-spectral efficiency (ESE), base station deployment, coordinated multi-point (CoMP), large-scale users' behaviors (LSUBs).

## I. INTRODUCTION

THE operational mobile communication network is already capable of accommodating a massive number of high

Manuscript received 4 May 2023; revised 5 November 2023; accepted 8 November 2023. Date of publication 10 November 2023; date of current version 22 April 2024. The work of Lajos Hanzo was supported in part by Engineering and Physical Sciences Research Council Projects under Grants EP/W016605/1, EP/X01228X/1, and EP/Y026721/1 and in part by European Research Council's Advanced Fellow Grant QuantCom under Grant 789028. The review of this article was coordinated by Dr. Ai-Chun Pang. (*Corresponding author: Lajos Hanzo.*)

Guogang Zhao is with the School of Computer and Communication Engineering, Zhengzhou University of Light Industry, Zhengzhou 450066, China (e-mail: guogangzhao0125@163.com).

Sheng Chen and Lajos Hanzo are with the School of Electronics and Computer Science, University of Southampton, SO17 1BJ Southampton, U.K. (e-mail: sqc@ecs.soton.ac.uk; lh@ecs.soton.ac.uk).

Digital Object Identifier 10.1109/TVT.2023.3332028

throughput, low-latency services. However, improving the energy efficiency is of salient importance in approaching the ambitious net zero carbon emission target of the near future. A substantial amount of energy is dissipated by the base stations (BSs) both during signal transmission by the power amplifiers and by the associated cooling [1]. Thus, the network's energy dissipation is predominantly determined by the BS density and by the specific BS operations [2]. Energy efficient BS deployment has to obey the optimal BS density in the specific area based on the traffic volume, while maintaining high spectral efficiency. The term 'BS deployment' in this context refers to the specific positioning of the BSs and on how the BS sleep-mode is controlled.

### A. State-of-the-Art

It is widely recognized that an attractive mathematical tool conceived for investigating the BS allocation is constituted by stochastic geometry, which models the distribution of BSs by a Poisson point process (PPP) [3], [4], [5]. Recently, some authors also conceived energy efficient BS deployment strategies and analyzed the network's energy efficiency (EE) by relying on stochastic geometry [6], [7], [8], [9]. More specifically, the authors of [6] modeled and optimized the cellular network's EE. In [7], an energy efficient BS deployment strategy was proposed for hybrid RF/VLC networks. The authors of [8] analyzed the network's spectral efficiency (SE) and EE for a device-to-device communications aided millimeter-wave cellular network. In [9], energy efficient BS deployment relying on coverage range expansion was proposed. However, these studies are based on the assumption of a constant power consumption for each BS and they do not take into account the large-scale user behaviors (LSUBs), including the network's geographical mobile-traffic intensity and the users' average data rate, etc. The recent study in [10] proposed user-centric BS clustering and resource allocation for the joint BS clustering and resource allocation problem in ultra-dense heterogeneous cellular networks (HCN). However, no EE/SE optimization strategy was discussed. By contrast, Zhao et al. [2], [11] overcame the aforementioned problem. In particular, in [2], a mobile-traffic-aware BS deployment strategy was proposed to maximize the cellular network's EE, while meeting the users' outage probability requirements. Zhao et al. [11] also proposed a BS deployment strategy matching the

LSUBs in a HCN. However, none of the above-mentioned treatises considered sophisticated coordinated multi-point (CoMP) transmission for increasing the energy-efficiency of BS deployment.

Recently, several studies dedicated to CoMP-aided randomly deployed large-scale cellular networks and relying on stochastic geometry have emerged in the literature [12], [13], [14], [15], [16], [17]. The authors of [12] developed their stochastic geometry based CoMP analysis method for analyzing large-scale randomly deployed cellular networks. The study [13] proposed a generalized CoMP analysis model for deriving the system's outage probability and capacity. The authors of [14] conceived a 3D CoMP transmission scheme for a large-scale randomly deployed air-to-air network. As a further advance, the authors of [15] used stochastic geometry for analyzing CoMP-assisted transmission in the downlink (DL) of heterogeneous cloud radio access networks. In [16], a Poisson-Delaunay triangulation based approach was advocated for analyzing a CoMP system, while the authors of [17] developed a BS coordination scheme for multi-tier ultra-dense networks. However, all the existing studies assume a constant power consumption for each BS and they do not quantify the beneficial impact of intelligent inter-BS cooperation on the BS's energy and spectrum utilization as well as EE performance. By contrast, our previous work [18] overcame the above-mentioned problem by establishing the relationship between the EE of large-scale randomly deployed cellular networks and the inter-BS cooperation. However, jointly optimizing cross-tier CoMP and BS deployment, while simultaneously taking into account the LSUBs, is necessary in order to further enhance the energy-spectral-efficiency (ESE) of HCNs, which is quite challenging.

## B. Our Contributions

Our objective is to propose an ESE framework for large-scale CoMP-aided two-tier HCNs, which facilitates the joint analysis of the impact of per-tier CoMP activation factors, per-tier BS densities and the randomly time-varying LSUBs. We also consider the impact of the geographical mobile-traffic intensity and the load migration factor as well as the average required service rate per tier. Based on this framework, we develop the optimal design strategies to maximize the ESE of large-scale CoMP-aided two-tier HCNs, while taking into account the maximum tolerable outage probability constraints. Hence we explicitly answer the following pair of research questions: 1. Is it possible to obtain the optimal CoMP activation factors that maximize the network ESE? 2. Is it possible to increase the performance gain attained by the joint optimization of the CoMP activation factors and BS densities? Our contributions are summarized as follows.

1) *CoMP-Enhanced ESE Modeling*: We first introduce a pair of CoMP-factors for characterizing the degree of CoMP-style macrocell-tier and small-cell-tier collaboration, which may be flexibly adjusted to control the specific fraction of cell-edge users in each tier relying on the CoMP mode. Then a new BS transmission power evaluation model is constructed, which includes the LSUBs, the degree of inter-BS cooperation and the large-scale BS deployment parameters. We define and derive the

network's ESE, followed by a comprehensive insight into how the geographic mobile-traffic intensity, the average user-rate, the BS density, the CoMP activation factors and other cellular parameters influence the network's ESE.

2) *Tractable CoMP-Enhanced ESE Analysis*: Armed with our closed-form ESE expression, we then derive the optimum CoMP activation factors given the other system parameters, including the macro/small BS densities, the geographical mobile-traffic intensity and the average user rate. We find that there always exists a unique CoMP activation factor that maximizes the network's ESE under a specific inter-BS spectrum balance constraint. Similarly, by exploring the relationship of the ESE as a function of the macro/small BS densities, we demonstrate that there is only a single macro/small BS density pair, which optimizes the ESE. The closed-form nature of this ESE expression thus makes our search for the network ESE-based optimal solutions particularly efficient, enabling us to design the optimal solutions for dense large-scale CoMP-aided two-tier HCNs.

3) *Design Strategies*: We then proceed to derive an optimal cellular-scenario-aware inter-BS cooperation strategy with the aid of the above-mentioned efficient ESE analysis tool, which maximizes the network's ESE, while meeting specific outage probability constraints. Specifically, based on this network ESE analysis tool, we jointly optimize the CoMP activation factor and the macro/small BS densities, under specific outage probability constraints, in order to derive a mobile-traffic-aware joint CoMP and BS deployment strategy that maximizes the global ESE. We demonstrate that our joint design strategy significantly outperforms the stand-alone inter-BS cooperation strategy in terms of the achievable ESE.

Table I contrasts the proposed ESE optimization framework to the existing state-of-the-art.

## II. SYSTEM MODEL

Table II summarized the symbols used in this paper.

### A. Network Layout

Large numbers of macro-BSs, denoted by the set  $\Psi_m = \{m_i\}$ , and small-BSs, indicated by the set  $\Psi_s = \{s_j\}$ , are randomly deployed according to two independent homogeneous PPPs with densities  $\lambda_m$  and  $\lambda_s$ , respectively, in the Euclidean plane  $\mathbb{R}^2$ . Similarly, single-antenna user equipment (UE), denoted by the set  $\Psi_u$ , are spatially distributed in  $\mathbb{R}^2$  according to an independently homogeneous PPP with density  $\lambda_u$ , which are further classified into macro and small UE based on the type of associated BS. For simplicity of analysis, we assume that the transmission of BS to a UE is with single antenna, that is, we exclude the MIMO effect.

A typical UE  $u_o$  is served by a macro-BS when

$$\min_{m_i \in \Psi_m} \|u_o - m_i\| \leq \mu \min_{s_j \in \Psi_s} \|u_o - s_j\|, \quad (1)$$

and otherwise it associates with a small-BS if

$$\min_{m_i \in \Psi_m} \|u_o - m_i\| > \mu \min_{s_j \in \Psi_s} \|u_o - s_j\|, \quad (2)$$

TABLE I  
 CONTRASTING THE PROPOSED ESE OPTIMIZATION FRAMEWORK TO THE EXISTING STATE-OF-THE-ART

Method	ESE optimization	BS deployment	Utilizing LSUBs	Utilizing CoMP	For HCNs
Guo et al. 2013 [19]	×	✓	×	×	✓
Zhao et al. 2017 [18]	✓	✓	×	✓	✓
Renzo et al. 2018 [6]	×	✓	×	×	×
Zhao et al. 2018 [11]	✓	✓	✓	×	✓
Kong et al. 2019 [7]	×	✓	×	×	✓
Ochia et al. 2019 [8]	✓	×	×	×	✓
Tao et al. 2019 [9]	×	✓	×	×	✓
Elhatab et al. 2020 [15]	×	×	×	✓	✓
Li et al. 2020 [16]	×	✓	×	✓	×
Mukherjee et al. 2021 [17]	×	✓	×	✓	✓
Su et al. 2023 [10]	×	✓	×	×	✓
Proposed	✓	✓	✓	✓	✓

 TABLE II  
 LIST OF SYMBOLS

Notation	Definition
$\Psi_m, \Psi_s, \Psi_u$	Sets of macro BSs, small BSs, UE
$\lambda_m, \lambda_s, \lambda_u$	Densities of macro BSs, small BSs, UE
$V_{m_i}, V_{s_j}$	Cellular cells covered by macro BS $m_i$ , small BS $s_j$
$\Psi_{u,m_i}, \Psi_{u,s_j}$	Sets of UE in cells $V_{m_i}, V_{s_j}$
$\Psi_{u,m_i}^{NC}, \Psi_{u,s_j}^{NC}$	Sets of No-CoMP UE in $V_{m_i}, V_{s_j}$
$\Psi_{u,m_i}^C, \Psi_{u,s_j}^C$	Sets of CoMP UE in $V_{m_i}, V_{s_j}$
$\mu, \rho_0$	Inter-tier weight factor, $\rho_0 = 1/\mu$
$\rho_1, \rho_2$	Macro-CoMP-factor, small-CoMP-factor
$s_k^{CT}$	nearest small BS to CoMP $u_{m_i}^k \in \Psi_{u,m_i}^C$
$m_l^{CT}$	nearest macro BS to CoMP $u_{s_j}^l \in \Psi_{u,s_j}^C$
$u_{m_i}^{k'}, u_{s_j}^{l'}$	$u_{m_i}^{k'} \in \Psi_{u,m_i}^{NC}, u_{s_j}^{l'} \in \Psi_{u,s_j}^{NC}$
$u_{m_i}^k, u_{s_j}^l$	$u_{m_i}^k \in \Psi_{u,m_i}^C, u_{s_j}^l \in \Psi_{u,s_j}^C$
$B$	Total bandwidth resources available to a BS
$B_{c1}, B_{c1}^{out}$	Interior-, Outer-resources in macro BS $m_i$
$B_{c2}, B_{c2}^{out}$	Interior-, Outer-resources in small BS $s_j$
$N_i, N_j$	Number of subbands in $B_{c1}, B_{c2}$
$\alpha$	Pathloss exponent
$P_{k'}^{Tx}$	DL transmit power from $m_i$ to No-CoMP $u_{m_i}^{k'}$
$P_{k,1}^{Tx}, P_{k,2}^{Tx}$	DL transmit powers from $m_i, s_k^{CT}$ to CoMP $u_{m_i}^k$
$P_k^{Tx}$	$P_k^{Tx} = P_{k,1}^{Tx} + P_{k,2}^{Tx}$
$P_{l'}^{Tx}$	DL transmit power from $s_j$ to No-CoMP $u_{s_j}^{l'}$
$P_{l,1}^{Tx}, P_{l,2}^{Tx}$	DL transmit powers from $m_l^{CT}, s_j$ to CoMP $u_{s_j}^l$
$P_l^{Tx}$	$P_l^{Tx} = P_{l,1}^{Tx} + P_{l,2}^{Tx}$
$P_m, P_s$	Maximum DL BS transmit powers in $B_{c1}, B_{c2}$
$P_m^{TX}, P_s^{TX}$	Aggregate DL transmit powers in $V_{m_i}, V_{s_j}$
$P_{in}^m, P_{in}^s$	Maximum transmit (interference) power per subband from macro BS, small BS
$\eta_{ESE}$	Network's ESE metric
$Q_{out}$	Outage probability of Non-CoMP $u_{m_i}^{k'}$
$R_{max}$	Maximum rate threshold of $u_{m_i}^{k'}$
$A_m, A_s$	Coverage area of $V_{m_i}, V_{s_j}$
$\beta_m, \beta_s$	Power amplifier efficiency of macro BS, small BS
$P_{OM}^m, P_{OM}^s$	Circuit-dissipation power of macro BS, small BS
$\varepsilon_{out}$	Outage threshold

where  $\|\cdot\|$  denotes the Euclidean distance, and  $\mu > 0$  is the inter-tier weight factor. Physically,  $\mu$  is related to the mobile-traffic distribution at each tier. Generally, increasing  $\mu$  enables more UE to be served by macro-BSs and vice versa.

Thus the BS sets  $\Psi_m$  and  $\Psi_s$  form a weighted Voronoi tessellation model in  $\mathbb{R}^2$ , where  $V_{m_i}$  and  $V_{s_j}$  denote the coverage regions of macro-BS  $m_i$  and small-BS  $s_j$ , respectively.  $\mu$  is a long-term averaged quantity, where the fading is averaged out, and it is proportional to the ratio of the power-level received from macro-BS to the power level received from small-BS [20],

[21]. Since the power-level received from a macro-BS is much higher than that from a small-BS,  $\mu > 1$  is true. The macro UE or small UE are divided into two groups based on the mode selection, i.e., No-CoMP and CoMP mode. The UE in No-CoMP mode is served by only one BS. By contrast, for the UE operates in CoMP mode, the nearest BS in another tier and its originally serving BS will transmit desired signals in a coordinated manner to the UE. Since the geographical mobile-traffic intensity is proportional to the UE's spatial density  $\lambda_u$  given the average user rate requirement, we will use  $\lambda_u$  to equivalently represent the mobile-traffic intensity.

### B. Cross-Tier Inter-BS Cooperative Transmission Mechanism

We introduce a geographical cross-tier inter-BS cooperation mechanism for the large-scale DL CoMP-enabled two-tier HCN. The set of UE in the typical cell  $V_{m_i}$  ( $V_{s_j}$ ) is denoted by  $\Psi_{u,m_i}$  ( $\Psi_{u,s_j}$ ). The set of UE in the typical cell  $V_{m_i}$  ( $V_{s_j}$ ) is denoted by  $\Psi_{u,m_i}$  ( $\Psi_{u,s_j}$ ), in which  $\Psi_{u,m_i}^{NC}$  ( $\Psi_{u,s_j}^{NC}$ ) is the set of No-CoMP macro (small) UE and  $\Psi_{u,m_i}^C$  ( $\Psi_{u,s_j}^C$ ) is the set of CoMP macro (small) UE.

For a typical macro UE  $u_{m_i} \in \Psi_{u,m_i}$  with

$$r_0 = \|u_{m_i} - m_i\|, \quad (3)$$

$$r_1 = \min_{s_j \in \Psi_s} \|u_{m_i} - s_j\|, \quad (4)$$

$u_{m_i}$  operates in CoMP mode when  $\rho_0 < r_1/r_0 < \rho_1$ , i.e.,  $u_{m_i} \in \Psi_{u,m_i}^C$ . Note that  $\rho_1$  is a tunable parameter from the large-scale network perspective to control the cross-tier inter-BSSs cooperation degree for macro UE, i.e., it is the macro-CoMP-factor, which satisfies  $0 < \rho_0 < \rho_1$  with  $\rho_0 = 1/\mu$ . Assume that  $u_{m_i}$  is the  $k$ -th CoMP UE in  $\Psi_{u,m_i}^C$ , denoted by  $u_{m_i}^k$ . That is,  $\Psi_{u,m_i}^C = \{u_{m_i}^k\}$ . The macro BS  $m_i$  and the nearest small BS to  $u_{m_i}^k$ , denoted by  $s_k^{CT}$  which satisfies  $s_k^{CT} = \arg \min_{s_j \in \Psi_s} \|u_{m_i}^k - s_j\|$ , will coordinately transmit the desired signals for  $u_{m_i}^k$ . Otherwise, when  $r_1/r_0 > \rho_1$ ,  $u_{m_i}$  operates in No-CoMP mode, i.e.,  $u_{m_i} \in \Psi_{u,m_i}^{NC}$ . Let  $\Psi_{u,m_i}^{NC} = \{u_{m_i}^{k'}\}$ . Then only the macro BS  $m_i$  serves  $u_{m_i}^{k'}$ .

Similarly, for a typical small UE  $u_{s_j} \in \Psi_{u,s_j}$ , let

$$\bar{r}_0 = \min_{m_i \in \Psi_m} \|u_{s_j} - m_i\|, \quad (5)$$

$$\bar{r}_1 = \|u_{s_j} - s_j\|. \quad (6)$$

Then  $u_{s_j}$  operates in CoMP mode, i.e.,  $u_{s_j} \in \Psi_{u,s_j}^C$ , when  $1/\rho_1 < \bar{r}_0/\bar{r}_1 < 1/\rho_2$ . Assume that this small UE is the  $l$ -th CoMP small UE in  $\Psi_{u,s_j}^C$ , denoted by  $u_{s_j}^l$ . That is,  $\Psi_{u,s_j}^C = \{u_{s_j}^l\}$ . Then the nearest macro BS to  $u_{s_j}^l$ , denoted by  $m_l^{CT}$  which satisfies  $m_l^{CT} = \arg \min_{m_i \in \Psi_m} \|u_{s_j}^l - m_i\|$ , and the small BS  $s_j$  coordinately transmit the desired signals for  $u_{s_j}^l$ . Otherwise,  $u_{s_j} \in \Psi_{u,s_j}^{NC}$  if  $\bar{r}_0/\bar{r}_1 > \frac{1}{\rho_2}$ . Let this  $u_{s_j}$  be the  $l'$ -th No-CoMP in  $\Psi_{u,s_j}^{NC}$ , i.e.,  $\Psi_{u,s_j}^{NC} = \{u_{s_j}^{l'}\}$ . Then  $u_{s_j}^{l'}$  is only served by small BS  $s_j$ . Note that  $\rho_2$  defines the small-CoMP-factor which satisfies  $0 < \rho_2 < \rho_0$ .

We now define the probabilities of the typical macro-cell and small-cell UEs being supported in CoMP and No-CoMP mode, respectively, which are the part of the operational parameters in a large-scale CoMP-aided HCN.

*Lemma 1:* In a large-scale DL CoMP-aided two-tier HCN having a macro BS density of  $\lambda_m$ , small BSs density of  $\lambda_s$ , macro-CoMP-factor of  $\rho_1$  and small-CoMP-factor of  $\rho_2$ , the probability of a typical macro UE  $u_{m_i}$  to operate in CoMP mode is

$$p_{11} = \frac{\lambda_m}{\lambda_m + \lambda_s \rho_0^2} - \frac{\lambda_m}{\lambda_m + \lambda_s \rho_1^2}, \quad (7)$$

and the probability for  $u_{m_i}$  to operate in No-CoMP mode is

$$p_{10} = \frac{\lambda_m}{\lambda_m + \lambda_s \rho_1^2}. \quad (8)$$

Here  $0 < \rho_0 < \rho_1$  and  $\rho_0 = 1/\mu$ . On the other hand, the probability for a typical small UE  $u_{s_j}$  to operate in CoMP mode is given by

$$p_{21} = \frac{\lambda_s \rho_0^2}{\lambda_s \rho_0^2 + \lambda_m} - \frac{\lambda_s \rho_2^2}{\lambda_s \rho_2^2 + \lambda_m}, \quad (9)$$

while the probability for  $u_{s_j}$  to operate in No-CoMP mode is

$$p_{20} = \frac{\lambda_s \rho_2^2}{\lambda_s \rho_2^2 + \lambda_m}, \quad (10)$$

where  $0 < \rho_2 < \rho_0$ .

*Proof:* See Appendix A.  $\blacksquare$

### C. Resource Partitioning Under Cross-Tier Inter-BS Cooperative Transmission

The UE in the sets of  $\Psi_{u,m_i}$  and  $\Psi_{u,s_j}$  adopt the orthogonal time-frequency resources (e.g., OFDMA) and CoMP-enabled cross-tier partial universal frequency reuse. The total bandwidth of  $B$  Hz is allocated to a macro BS  $m_i$  (small BS  $s_j$ ). For the technical implementation details of CoMP, the reader is referred to for example [22].

For a macro cell  $\Psi_{m_i}$ , the bandwidth is divided into two parts as  $B = B_{c1} + B_{c1}^{\text{out}}$ . The first part  $B_{c1}$  forms the interior-resources, which can only be occupied by the UE in  $\Psi_{u,m_i}$ , and the second part  $B_{c1}^{\text{out}}$ , referred to as the outer-resources, exclusively serve the small CoMP UE in the closest small cells that need to cooperate with  $m_i$ . Similarly, the bandwidth of a small cell  $\Psi_{s_j}$  is divided as  $B = B_{c2} + B_{c2}^{\text{out}}$ . The interior-resources  $B_{c2}$  can only be occupied by the UE in  $\Psi_{u,s_j}$ , while

the outer-resources  $B_{c2}^{\text{out}}$  exclusively serve the macro CoMP UE in the closest macro cells that need to cooperate with  $s_j$ .

In our work, only a statistical channel state information is required for CoMP operation to obtain multiple cellular diversity gains, such as the open loop non-coherent joint transmission [12]. From Lemma 1, the average percentage of the small CoMP UE over the total small UE in this large-scale CoMP-enabled two-tier HCN can be expressed as the probability  $\Pr(\text{percentage of CoMP small UE}) = \frac{p_{21}}{p_{20} + p_{21}}$ . This probability can be considered the one that a typical macro BS is forced by small BSs for CoMP. Therefore, each macro BS must provide the system bandwidth for the small CoMP UE as  $E[B_{c1}^{\text{out}}] = \frac{p_{21}}{p_{20} + p_{21}} B$  on average, where  $E[\cdot]$  denotes the expectation operator. Similarly, each small BS must provide the bandwidth  $E[B_{c2}^{\text{out}}] = \frac{p_{11}}{p_{10} + p_{11}} B$  for the macro CoMP UE on average. Naturally, increasing the small CoMP factor  $\rho_2$  can increase the consumption of  $B_{c1}^{\text{out}}$  and vice versa. Since  $B = B_{c1} + B_{c1}^{\text{out}}$  and  $B = B_{c2} + B_{c2}^{\text{out}}$ , we have  $E[B_{c1}] = \frac{p_{20}}{p_{20} + p_{21}} B$  and  $E[B_{c2}] = \frac{p_{10}}{p_{10} + p_{11}} B$  for a typical macro cell and small cell, respectively. Focusing on a typical macro cell  $V_{m_i}$  with  $\lambda_s/\lambda_m$  small BSs underlaid averagely, then  $B_{c1}^{\text{out}}$  should be equal to the sum of all the resources used by small UE for CoMP in  $V_{m_i}$ . This implicit relationship can be mathematically expressed as  $E[B_{c1}^{\text{out}}] \frac{\lambda_s}{\lambda_m} = E[B_{c2}^{\text{out}}]$ .

Specifically, the total bandwidth resource  $B$  of a macro cell  $\Psi_{m_i}$  is equally divided into a number of orthogonal time-frequency resource blocks. The  $\frac{p_{20}}{p_{20} + p_{21}}$  proportion of these equal-size resource blocks are assigned to the UE in  $\Psi_{u,m_i}$ , and the  $\frac{p_{21}}{p_{20} + p_{21}}$  proportion of them are reserved for the small CoMP UE in the closest small cells. In the same way, the total bandwidth resource  $B$  of a small cell  $\Psi_{s_j}$  is equally divided into a number of orthogonal time-frequency resource blocks. The  $\frac{p_{10}}{p_{10} + p_{11}}$  proportion of these resource blocks is then assigned to the UE in  $\Psi_{u,s_j}$ , and the  $\frac{p_{11}}{p_{10} + p_{11}}$  proportion of them are reserved for the macro CoMP UE in the closest macro cells.

The  $k$ -th macro CoMP UE  $u_{m_i}^k$  in  $\Psi_{u,m_i}$  is simultaneously served by its macro BS  $m_i$  and its nearest small BS  $s_k^{CT}$ . Hence both the macro BS  $m_i$  and the collaborating small BS  $s_k^{CT}$  must assign the same resource block to the macro CoMP UE  $u_{m_i}^k$ , which will come from the interior-resources of  $m_i$  and the outer-resources of  $s_k^{CT}$ , respectively. In this way, the strongest cross-tier interference from  $s_k^{CT}$  becomes useful information for  $u_{m_i}^k$ . Similarly, the  $l$ -th small CoMP UE  $u_{s_j}^l$  in  $\Psi_{u,s_j}$  will be assigned a common subband by both its serving small BS  $s_j$  and its CoMP serving macro BS  $m_l^{CT}$ .

### D. Power Consumption Modeling Under Cross-Tier Inter-BS Cooperative Transmission

For the DL from macro BS  $m_i$  to No-CoMP macro UE  $u_{m_i}^{k'}$ , which requires the service rate of  $R_{k'}$  in its allocated resource  $B_{k'}$ , the DL transmit power  $P_{k'}^{Tx}$  satisfies

$$R_{k'} = B_{k'} \log_2 \left( 1 + \frac{P_{k'}^{Tx} L_{k'}^i h_{k'}^i}{I_{k'}} \right), \quad (11)$$

where  $L_{k'}^i$  is the large-scale path-loss between  $m_i$  and  $u_{m_i}^{k'}$ ,  $h_{k'}^i$  is the fast-fading channel gain from  $m_i$  to  $u_{m_i}^{k'}$ , and

$$I_{k'} = \sum_{m_{i'} \in \{\Psi_m \setminus m_i\}} P_{\text{In}}^m L_{k'}^{i'} h_{k'}^{i'} + \sum_{s_j \in \Psi_s} P_{\text{In}}^s L_{k'}^j h_{k'}^j \quad (12)$$

is the interference power, in which  $L_{k'}^j$  is the large-scale path-loss between small BS  $s_j$  and No-CoMP macro UE  $u_{m_i}^{k'}$  and  $h_{k'}^j$  is the fast-fading channel gain from  $s_j$  to  $u_{m_i}^{k'}$ , while  $P_{\text{In}}^m$  and  $P_{\text{In}}^s$  are the maximum transmit powers of macro BS and small BS, respectively, in this resource block  $B_{k'}$ . The fast-fading channel gain follows the independent exponential distribution with unity mean [3], i.e.,  $h_{k'}^i, h_{k'}^j \sim \exp(1)$ . Similarly, for a typical CoMP macro UE  $u_{m_i}^k$ , which requires the service rate of  $R_k$  in its allocated resource  $B_k$ , we have

$$R_k = B_k \log_2 \left( 1 + \frac{P_{k,1}^{Tx} L_k^i h_k^i + P_{k,2}^{Tx} L_k^{CT} h_k^{CT}}{I_k} \right), \quad (13)$$

where  $L_k^{CT}$  and  $h_k^{CT}$  are respectively the path-loss and fast-fading gain from the serving small BS  $s_k^{CT}$  to  $u_{m_i}^k$ ,  $P_{k,1}^{Tx}$  and  $P_{k,2}^{Tx}$  denote the DL transmit powers from  $m_i$  and  $s_k^{CT}$  to  $u_{m_i}^k$ , respectively, while the interference power is given by

$$I_k = \sum_{m_{i'} \in \{\Psi_m \setminus m_i\}} P_{\text{In}}^m L_k^{i'} h_k^{i'} + \sum_{s_j \in \{\Psi_s \setminus s_k^{CT}\}} P_{\text{In}}^s L_k^j h_k^j. \quad (14)$$

For the  $l'$ -th small No-CoMP UE  $u_{s_j}^{l'}$  with the resource  $B_{l'}$  and DL transmit power  $P_{l'}^{Tx}$ , its service rate is

$$R_{l'} = B_{l'} \log_2 \left( 1 + \frac{P_{l'}^{Tx} L_{l'}^j h_{l'}^j}{I_{l'}} \right), \quad (15)$$

where  $L_{l'}^j$  and  $h_{l'}^j$  are the large-scale path-loss and fast-fading channel gain between  $s_j$  and  $u_{s_j}^{l'}$ , respectively, and the interference power is given by

$$I_{l'} = \sum_{m_i \in \Psi_m} P_{\text{In}}^m L_{l'}^i h_{l'}^i + \sum_{s_{j'} \in \{\Psi_s \setminus s_j\}} P_{\text{In}}^s L_{l'}^{j'} h_{l'}^{j'}, \quad (16)$$

in which  $L_{l'}^i$  and  $h_{l'}^i$  are the large-scale path-loss and fast-fading channel gain between macro BS  $m_i$  and small UE  $u_{s_j}^{l'}$ , respectively. For the  $l$ -th small CoMP UE  $u_{s_j}^l$  with the resource  $B_l$ , its service rate is

$$R_l = B_l \log_2 \left( 1 + \frac{P_{l,1}^{Tx} L_l^{CT} h_l^{CT} + P_{l,2}^{Tx} L_l^j h_l^j}{I_l} \right), \quad (17)$$

where  $L_l^{CT}$  and  $h_l^{CT}$  are respectively the path-loss and fast-fading gain from the collaborating macro BS  $m_l^{CT}$  to  $u_{s_j}^l$ ,  $P_{l,1}^{Tx}$  and  $P_{l,2}^{Tx}$  denote the DL transmit powers from  $m_l^{CT}$  and  $s_j$  to  $u_{s_j}^l$ , respectively, while the interference power is

$$I_l = \sum_{m_i \in \{\Psi_m \setminus m_l^{CT}\}} P_{\text{In}}^m L_l^i h_l^i + \sum_{s_{j'} \in \{\Psi_s \setminus s_j\}} P_{\text{In}}^s L_l^{j'} h_l^{j'}. \quad (18)$$

Unless noted otherwise, the impact of channel noise is ignored, since the interference power experienced by a UE is far higher than the noise power in an interference-limited scenario. Also the interference powers (12), (14), (16) and (18) represent

the worst-case scenarios, and hence the specified DL transmit powers can guarantee the corresponding service rates.

We then define the aggregate DL macro cell transmit power as the sum of the transmit powers consumed in the transmission to all the macro UE in  $\Psi_{u,m_i}$ , which is

$$P_m^{TX} = \sum_{u_{m_i}^{k'} \in \Psi_{u,m_i}^{NC}} P_{k'}^{Tx} + \sum_{u_{m_i}^k \in \Psi_{u,m_i}^C} (P_{k,1}^{Tx} + P_{k,2}^{Tx}). \quad (19)$$

$P_m^{TX}$  is randomly varying in practice depending on many factors but is predominately influenced by the mobile-traffic load and average user rate. Similarly, the aggregate DL small cell transmit power is given by

$$P_s^{TX} = \sum_{u_{s_j}^{l'} \in \Psi_{u,s_j}^{NC}} P_{l'}^{Tx} + \sum_{u_{s_j}^l \in \Psi_{u,s_j}^C} (P_{l,1}^{Tx} + P_{l,2}^{Tx}). \quad (20)$$

Our formulation of  $P_m^{TX}$  and  $P_s^{TX}$  specifically takes into account the impact of mobile-traffic intensity  $\lambda_u$ .

### E. Performance Metrics

We continue by defining the network-level ESE metric as

$$\eta_{ESE} = \frac{\text{NT}}{\text{ARC}} \text{ [bps/(watt} \cdot \text{Hz)]}, \quad (21)$$

where ‘NT’ refers to the sum of the users’ average service rates per unit area measured in [bit/s/m<sup>2</sup>], and the area resource consumption (ARC) is the sum of the resource consumptions per unit area [(watt · Hz)/m<sup>2</sup>]. When deriving the ESE, we can adopt the general power consumption model for each BS specified by the standards organizations [23].

Next we define the outage probability for a typical No-CoMP macro UE  $u_{m_i}^{k'}$  as

$$Q_{out} = \Pr(R_{\max} < R_{k'}), \quad (22)$$

which is the probability that the maximum data rate threshold, denoted by  $R_{\max} = B_{k'} \log_2(1 + P_{\text{In}}^m/I_{k'})$ , is smaller than the required data rate of  $u_{m_i}^{k'}$ . Note that the outage probability of a CoMP UE will be lower than that of a typical No-CoMP UE, which is served simultaneously by two BSs. Our main focus is the ESE evaluation for a large-scale CoMP-enhanced two-tier HCN and, therefore, the outage probabilities of No-CoMP macro UE are used as constraints.

## III. ENERGY-SPECTRAL EFFICIENCY OF LARGE-SCALE TWO-TIER HCN WITH CROSS-TIER INTER-BS COOPERATIVE TRANSMISSION

In this section, we derive the ESE for the large-scale two-tier HCN with cross-tier inter-BS cooperative transmission, having macro-BS density  $\lambda_m$ , small BS-density  $\lambda_s$ , mobile-traffic intensity  $\lambda_u$ , macro-CoMP factor  $\rho_1$  and small-CoMP factor  $\rho_2$ . The ESE is a function of the average DL transmit powers for both typical macro (small) CoMP UE and typical macro (small) No-CoMP UE as well as the average aggregate DL transmit powers in typical macro-cell and small-cell.

### A. Average DL Transmit Power of Typical Macro (Small) No-CoMP (CoMP) UE

Typical No-CoMP macro UE's DL transmit power is first given in the following proposition.

*Proposition 1:* The average DL transmit power of macro BS  $m_i$  to typical No-CoMP macro UE  $u_{m_i}^{k'}$  requiring service rate  $R_{k'}$  and associated with an interior subband  $B_{k'}$  of  $B_{c1}$  is given by

$$E[P_{k'}^{Tx}] = \frac{2\lambda_m(\lambda_m + \lambda_s\rho_0^2)}{(\alpha - 2)\lambda_u} \left(2^{R_{k'}/B_{k'}} - 1\right) \times \frac{(\lambda_m P_m + \lambda_s P_s \rho_1^{2-\alpha})}{(\lambda_m + \lambda_s \rho_1^2)^2}, \quad (23)$$

where  $\alpha > 2$  is the pathloss exponent,  $P_m = N_i P_{In}^m$  and  $P_s = N_j P_{Is}^m$  are the maximum DL BS transmit powers in  $B_{c1}$  and  $B_{c2}$ , respectively, while  $N_i$  and  $N_j$  are the numbers of the resource blocks or subbands contained in the interior-resources  $B_{c1}$  and  $B_{c2}$ , respectively.

*Proof:* See Appendix B. ■

From (23), the impact of the macro CoMP factor  $\rho_1$  on the average DL transmit power  $E[P_{k'}^{Tx}]$  can be revealed. Obviously,  $E[P_{k'}^{Tx}]$  contains the factor of  $\rho_1^{2-\alpha}$  in the numerator and  $\rho_1^4$  in the denominator. This indicates that  $E[P_{k'}^{Tx}]$  is a monotonically decreasing function of  $\rho_1$ . From Lemma 1, the probability  $p_{11}$  of macro UE operating in CoMP is increased upon improving  $\rho_1$ , and consequently the remaining No-CoMP UE will have a reduced distance ratio  $r_1/r_0$  and thus require less DL transmit power.

We next consider the average DL transmit power of a typical CoMP macro UE served by two cooperative BSs.

*Proposition 2:* The average total DL transmit power for typical macro CoMP UE  $u_{m_i}^k$  requiring service rate  $R_k$  as well as associated with the interior subband  $B_k$  of  $B_{c1}$  in macro-BS  $m_i$  and the outer subband  $B_k$  of  $B_{c2}^{\text{Out}}$  in small BS  $s_k^{CT}$  is given by

$$E[P_k^{Tx}] = \frac{(2^{R_k/B_k} - 1)(\lambda_m + \lambda_s \rho_0^2)}{(\alpha - 2)\lambda_u} \sum_{n'=1}^4 \mathcal{A}_{n'}, \quad (24)$$

where  $P_k^{Tx} = P_{k,1}^{Tx} + P_{k,2}^{Tx}$ ,

$$\mathcal{A}_1 = \frac{\lambda_m^2 P_m}{(\lambda_m + \lambda_s \rho_0^2)^2} - \frac{\lambda_m^2 P_m}{(\lambda_m + \lambda_s \rho_1^2)^2}, \quad (25)$$

$$\mathcal{A}_2 = \frac{4\lambda_m \lambda_s^2 P_s}{(\alpha + 2)} \left( \frac{\rho_0^{4-\alpha} {}_2F_1\left(1, 3; \frac{\alpha}{2} + 2; \frac{\lambda_m}{\lambda_m + \lambda_s \rho_0^2}\right)}{(\lambda_m + \lambda_s \rho_0^2)^3} - \frac{\rho_1^{4-\alpha} {}_2F_1\left(1, 3; \frac{\alpha}{2} + 2; \frac{\lambda_m}{\lambda_m + \lambda_s \rho_1^2}\right)}{(\lambda_m + \lambda_s \rho_1^2)^3} \right), \quad (26)$$

$$\mathcal{A}_3 = \frac{4\lambda_s \lambda_m^2 P_m}{(\alpha + 2)} \left( \frac{\rho_1^{\alpha+2} {}_2F_1\left(1, 3; \frac{\alpha}{2} + 2; \frac{\lambda_s \rho_1^2}{\lambda_s \rho_1^2 + \lambda_m}\right)}{(\lambda_m + \lambda_s \rho_1^2)^3} - \frac{\rho_0^{\alpha+2} {}_2F_1\left(1, 3; \frac{\alpha}{2} + 2; \frac{\lambda_s \rho_0^2}{\lambda_s \rho_0^2 + \lambda_m}\right)}{(\lambda_m + \lambda_s \rho_0^2)^3} \right), \quad (27)$$

$$\mathcal{A}_4 = \frac{\lambda_s^2 P_s \rho_1^4}{(\lambda_m + \lambda_s \rho_1^2)^2} - \frac{\lambda_s^2 P_s \rho_0^4}{(\lambda_m + \lambda_s \rho_0^2)^2}, \quad (28)$$

and  ${}_2F_1(\cdot, \cdot; \cdot; \cdot)$  is the Gauss hypergeometric function [24].

*Proof:* See Appendix C. ■

By considering both the No-CoMP and CoMP cases for typical macro UE  $u_{m_i}$ , the following corollary is obtained.

*Corollary 1:* The average DL transmit power for typical macro-UE  $u_{m_i}$ , denoted by  $E[P_{\text{MÜ}}^{Tx}]$ , is given by

$$E[P_{\text{MÜ}}^{Tx}] = \frac{p_{10}}{p_{10} + p_{11}} E[P_{k'}^{Tx}] + \frac{p_{11}}{p_{10} + p_{11}} E[P_k^{Tx}] = \frac{(\lambda_m + \lambda_s \rho_0^2)}{(\alpha - 2)\lambda_u} \frac{\left(2^{\frac{N_i R_{m_i}}{B_{c1}}} - 1\right)}{(p_{10} + p_{11})} \left(p_{10} \mathcal{A}_0 + p_{11} \sum_{n'=1}^4 \mathcal{A}_{n'}\right), \quad (29)$$

where  $R_{m_i}$  is the average of  $R_{k'}$  and  $R_k$ , and  $\mathcal{A}_0$  is given by

$$\mathcal{A}_0 = \frac{2\lambda_m(\lambda_m P_m + \lambda_s P_s \rho_1^{2-\alpha})}{(\lambda_m + \lambda_s \rho_1^2)^2}. \quad (30)$$

Next, we consider typical No-CoMP and CoMP small UE.

*Proposition 3:* The average DL transmit power of small BS  $s_j$  to typical No-CoMP small UE  $u_{s_j}^{l'}$  requiring service rate  $R_{l'}$  and associated with the interior subband  $B_{l'}$  of  $B_{c2}$  is given by

$$E[P_{l'}^{Tx}] = \frac{2\lambda_s \rho_2^4 (\lambda_s + \lambda_m / \rho_0^2)}{\lambda_u (\alpha - 2)} \left(2^{R_{l'}/B_{l'}} - 1\right) \times \frac{(\lambda_s P_s + \lambda_m P_m \rho_2^{2-\alpha})}{(\lambda_m + \lambda_s \rho_2^2)^2}. \quad (31)$$

*Proof:* See Appendix D. ■

Clearly,  $E[P_{l'}^{Tx}]$  is a monotonically decreasing function of  $\rho_2$ .

*Proposition 4:* The average total DL transmit power for typical small CoMP UE  $u_{s_j}^l$  requiring service rate  $R_l$ , associated with the interior subband  $B_l$  of  $B_{c2}$  in small-BS  $s_j$  and the outer subband  $B_l$  of  $B_{c1}^{\text{Out}}$  in macro BS  $m_l^{CT}$  is given by

$$E[P_l^{Tx}] = \frac{(2^{R_l/B_l} - 1)}{\lambda_u (\alpha - 2)} \left(\lambda_s + \frac{\lambda_m}{\rho_0^2}\right) \sum_{n'=1}^4 \mathcal{B}_{n'}, \quad (32)$$

where  $P_l^{Tx} = P_{l,1}^{Tx} + P_{l,2}^{Tx}$ ,

$$\mathcal{B}_1 = \lambda_s^2 P_s \left( \frac{\rho_0^4}{(\lambda_m + \lambda_s \rho_0^2)^2} - \frac{\rho_2^4}{(\lambda_m + \lambda_s \rho_2^2)^2} \right), \quad (33)$$

$$\mathcal{B}_2 = \frac{4\lambda_s \lambda_m^2 P_m}{\alpha + 2} \left( \frac{\rho_0^{\alpha+2} {}_2F_1\left(1, 3; \frac{\alpha}{2} + 2; \frac{\lambda_s \rho_0^2}{\lambda_m + \lambda_s \rho_0^2}\right)}{(\lambda_m + \lambda_s \rho_0^2)^3} - \frac{\rho_2^{\alpha+2} {}_2F_1\left(1, 3; \frac{\alpha}{2} + 2; \frac{\lambda_s \rho_2^2}{\lambda_m + \lambda_s \rho_2^2}\right)}{(\lambda_m + \lambda_s \rho_2^2)^3} \right), \quad (34)$$

$$\mathcal{B}_3 = \frac{4\lambda_m \lambda_s^2 P_s}{\alpha + 2} \left( \frac{\rho_2^{4-\alpha} {}_2F_1\left(1, 3; \frac{\alpha}{2} + 2; \frac{\lambda_m}{\lambda_m + \lambda_s \rho_2^2}\right)}{(\lambda_m + \lambda_s \rho_2^2)^3} - \frac{\rho_0^{4-\alpha} {}_2F_1\left(1, 3; \frac{\alpha}{2} + 2; \frac{\lambda_m}{\lambda_m + \lambda_s \rho_0^2}\right)}{(\lambda_m + \lambda_s \rho_0^2)^3} \right)$$

$$-\frac{\rho_0^{4-\alpha} {}_2F_1\left(1, 3; \frac{\alpha}{2} + 2; \frac{\lambda_m}{\lambda_m + \lambda_s \rho_0^2}\right)}{(\lambda_m + \lambda_s \rho_0^2)^3}, \quad (35)$$

$$\mathcal{B}_4 = \frac{\lambda_m^2 P_m}{(\lambda_m + \lambda_s \rho_0^2)^2} - \frac{\lambda_m^2 P_m}{(\lambda_m + \lambda_s \rho_0^2)^2}, \quad (36)$$

and again  ${}_2F_1(\cdot, \cdot; \cdot; \cdot)$  is the Gauss hypergeometric function [24].

*Proof:* See Appendix E. ■

By considering both the No-CoMP and CoMP cases for typical small UE  $u_{s_j}$ , we obtain the following corollary.

*Corollary 2:* The average DL transmit power for typical small-UE  $u_{s_j}$ , denoted by  $E[P_{\text{SU}}^{Tx}]$ , is given by

$$\begin{aligned} E[P_{\text{SU}}^{Tx}] &= \frac{p_{20}}{p_{20} + p_{21}} E[P_V^{Tx}] + \frac{p_{21}}{p_{20} + p_{21}} E[P_l^{Tx}] \\ &= \frac{2^{-\frac{N_j R_{s_j}}{B_{c2}}} \left(\lambda_s + \frac{\lambda_m}{\rho_0^2}\right)}{(\alpha - 2)(p_{20} + p_{21}) \lambda_u} \left(p_{20} \mathcal{B}_0 + p_{21} \sum_{n'=1}^4 \mathcal{B}_{n'}\right), \end{aligned} \quad (37)$$

where  $R_{s_j}$  is the average of  $R_V$  and  $R_l$ , and  $\mathcal{B}_0$  is given by

$$\mathcal{B}_0 = \frac{2\lambda_s \rho_0^4 (\lambda_s P_s + \lambda_m P_m \rho_0^{2-\alpha})}{(\lambda_m + \lambda_s \rho_0^2)^2}. \quad (38)$$

### B. Average Aggregate DL Transmit Power in Typical Macrocell (Small-Cell)

We consider the rate allocation between No-CoMP and CoMP UE in typical macro-cell and small-cell, where all the No-CoMP macro (small) UE and CoMP macro (small) UE have an identical rate of  $R_m$  ( $R_s$ ). Then the averaged aggregate DL transmit power in typical macro-cell and small-cell can be given in the following proposition.

*Proposition 5:* The averaged aggregate macro DL transmit power  $E[P_m^{TX}]$  within typical macro cell  $V_{m_i}$  is given by

$$\begin{aligned} E[P_m^{TX}] &= \frac{p_{10} \mathcal{A}_0 + p_{11} \sum_{n'=1}^4 \mathcal{A}_{n'}}{(p_{10} + p_{11})(\alpha - 2)} \\ &\times \left( \frac{K^K (\lambda_m + \lambda_s \rho_0^2)^K}{\left(K (\lambda_m + \lambda_s \rho_0^2) - \left(2^{\frac{R_m}{B_{c1}}} - 1\right) \lambda_u\right)^K} - 1 \right), \end{aligned} \quad (39)$$

where  $K = 3.75$ . The averaged aggregate small DL transmit power  $E[P_s^{TX}]$  within typical small cell  $V_{s_j}$  is given by

$$\begin{aligned} E[P_s^{TX}] &= \frac{p_{20} \mathcal{B}_0 + p_{21} \sum_{n'=1}^4 \mathcal{B}_{n'}}{(p_{20} + p_{21})(\alpha - 2)} \\ &\times \left( \frac{K^K (\lambda_s + \lambda_m / \rho_0^2)^K}{\left(K (\lambda_s + \lambda_m / \rho_0^2) - \left(2^{\frac{R_s}{B_{c2}}} - 1\right) \lambda_u\right)^K} - 1 \right). \end{aligned} \quad (40)$$

*Proof:* See Appendix F. ■

### C. Large-Scale Two-Tier HCN's ESE Metric With Cross-Tier Inter-BS Cooperative Transmission

Based on the above analytical results, we derive the network-level ESE metric. The ARC of a large-scale CoMP-enabled HCN with cross-tier inter-BS enhanced is given by

$$\begin{aligned} \text{ARC} &= \underbrace{B}_{\text{Bandwidth resource}} \times \left( \underbrace{\lambda_m (\beta_m E[P_m^{TX}] + P_{OM}^m)}_{\text{Macro energy resource: ARC}_m} \right. \\ &\quad \left. + \underbrace{\lambda_s (\beta_s E[P_s^{TX}] + P_{OM}^s)}_{\text{Small energy resource: ARC}_s} \right) [(\text{watt} \cdot \text{Hz}) / \text{m}^2], \end{aligned} \quad (41)$$

where  $\beta_m$  and  $\beta_s$  are the power amplifier efficiency of macro BS and small BS, respectively,  $P_{OM}^m$  and  $P_{OM}^s$  are the circuit-dissipation power, including the baseband signal processing, battery backup, BS cooling, etc., of macro BS and small BS, respectively. Next the network throughput is expressed by

$$\text{NT} = \underbrace{(p_{10} + p_{11}) R_m \lambda_u}_{\text{Macro UE}} + \underbrace{(p_{20} + p_{21}) R_s \lambda_u}_{\text{Small UE}} [\text{bit/s/m}^2]. \quad (42)$$

Based on the definition of (21) and the above-mentioned analytical results, the following proposition is obvious.

*Proposition 6:* The ESE of a large-scale CoMP-enhanced two-tier HCN can be expressed in the closed-form expressions of (43) to (45) shown at the bottom of the next page.

Note that owing to the identical equality of  $E[B_{c1}^{\text{Out}}] \frac{\lambda_s}{\lambda_m} = E[B_{c2}^{\text{Out}}]$ , the small CoMP factor  $\rho_2$  can be expressed as the function of the macro CoMP factor  $\rho_1$  as

$$\rho_2 = f(\rho_1) = \sqrt{\frac{\lambda_m (1 - \lambda_m (\rho_1^2 - \rho_0^2) / (\lambda_m + \lambda_s \rho_1^2))}{\frac{\lambda_m}{\rho_0^2} + \lambda_s \lambda_m (\rho_1^2 - \rho_0^2) / (\lambda_m + \lambda_s \rho_1^2)}}. \quad (46)$$

## IV. JOINT ESE OPTIMIZATION OF CROSS-TIER INTER-BS COOPERATION AND BS DEPLOYMENT

With the aid of the analytical results from the previous sections, we formulate two energy-spectral efficient design strategies for the large-scale two-tier CoMP-enhanced HCN.

### A. Cellular-Scenario-Aware Cross-Tier Inter-BS Cooperation Optimization Under Outage Performance Constraint

We introduce a cross-tier inter-BS cooperation optimization problem while satisfying all UE's quality of service (QoS) constraints. Specifically, we maximize the network ESE metric by choosing a pair of suitable macro and small CoMP factors, while guaranteeing the users' outage performance. The ESE metric's dependence on the degree of cross-tier inter-BS cooperation is illustrated in the following proposition. Note that we directly use macro CoMP factor  $\rho_1$  to characterize the degree of cross-tier inter-BS cooperation degree throughout network by applying the equality of (46).

*Proposition 7:* There exists a unique optimal macro/small-CoMP factor pair, denoted by  $(\rho_1^*, \rho_2^*)$ , which maximizes the

network's ESE metric of (43), which can be numerically obtained by solving the (47) shown at the bottom of this page.

The proof of Proposition 7 is straightforward by setting the gradient of the ESE metric with respect to  $\rho_1$  to zero and noting  $\rho_2$  (46) is a function of  $\rho_1$ .

We continue by analyzing the outage probability constraint. Note that the outage probability for a typical CoMP UE is much lower than that of typical No-CoMP UE in both macro and small cells, and moreover the outage probability for a macro UE is also lower than that of a small UE with a wider bandwidth. Therefore we focus on the outage performance for typical macro No-CoMP UE as the outage performance threshold, which is specified in the following proposition.

**Proposition 8:** The outage probability for typical macro No-CoMP UE  $u_{m_i}^{k'}$  requesting rate  $R_{k'}$  in subband  $B_{k'}$  and conditioned on  $r_0$  is given by

$$Q_{out}(r_0) = 1 - \exp\left(-\pi r_0^2 \lambda_m \sigma - \pi \mu^{-2/\alpha} r_0^2 \lambda_s \sigma\right), \quad (48)$$

where  $\sigma = T^{2/\alpha} \int_{T^{-2/\alpha}}^{+\infty} \frac{1}{1+u^{\alpha/2}} du$  and  $T = 2^{R_{k'}/B_{k'}} - 1$ . By applying  $E[N_i] = \frac{\lambda_u}{\lambda_m}$  and the average macro cell radius  $\approx \frac{1}{\sqrt{\pi \lambda_m}}$  as well as  $R_{k'} = R_m$  and  $B_{k'} = B_{c1}(\lambda_m + \lambda_s \rho_0^2)/\lambda_u$ , we obtain the average cellular outage probability as

$$Q_{out} = 1 - \exp\left(-\left(1 + \frac{\lambda_s}{\lambda_m} \mu^{-2/\alpha}\right) \sigma\right). \quad (49)$$

The proof for this proposition is similar to the proof of Proposition 8 in [18], and therefore it is omitted. Clearly the average cellular outage probability  $Q_{out}$  is a function of  $\rho_1$  and  $\rho_2$  as well as  $\lambda_m$ ,  $\lambda_s$  and  $\lambda_u$ . In the sequel, we also denote it as  $Q_{out}(\rho_1, \rho_2; \lambda_m, \lambda_s, \lambda_u)$ . Note that here we have

$$T = 2^{\frac{\lambda_u R_m}{B_{c1}(\lambda_m + \lambda_s \rho_0^2)}} - 1. \quad (50)$$

By combining the analytical results of Propositions 7 and 8, we formulate an ESE-orient cellular-scenario-aware cross-tier

inter-BS cooperation degree optimization problem (BPwCo) with the average cellular outage performance constraint. More specifically, the BPwCo is formulated as

$$\max_{\rho_1, \rho_2} \eta_{ESE}(\rho_1, \rho_2; \lambda_m, \lambda_s, \lambda_u), \quad (51)$$

$$\text{s.t. } 1 - \exp\left(-\left(1 + \frac{\lambda_s}{\lambda_m} \mu^{-2/\alpha}\right) \sigma\right) \leq \varepsilon_{out}, \quad (52)$$

$$0 < \rho_2 = f(\rho_1) < \rho_0 < \rho_1, \rho_0 = 1/\mu < 1, \quad (53)$$

where  $0 < \varepsilon_{out} < 1$  is the tolerable outage probability.

We now derive the optimal cross-tier inter-BS cooperation degree solution of the BPwCo, i.e., the optimal macro CoMP factor denoted as  $\rho_{1,out}^*$ . Let  $X = \lambda_m(\rho_1^2 - \rho_0^2)/(\lambda_m + \lambda_s \rho_1^2)$ . Then the derivative of  $\rho_2$  in (46) with respect to  $\rho_1^2$  satisfies

$$\frac{\partial \rho_2}{\partial(\rho_1^2)} = \frac{\partial \rho_2}{\partial X} \frac{\partial X}{\partial(\rho_1^2)} < 0, \quad (54)$$

due to  $\frac{\partial \rho_2}{\partial X} < 0$  and

$$\frac{\partial X}{\partial(\rho_1^2)} = \frac{\lambda_m^2 + \lambda_m \lambda_s \rho_0^2}{(\lambda_m + \lambda_s \rho_1^2)^2} > 0, \quad (55)$$

which implies that  $\rho_2$  is a monotonically decreasing function with respect to  $\rho_1^2$ . Based on the results of Section II-C,

$$E[B_{c1}] = \frac{\rho_2^2}{\lambda_s \rho_2^2 + \lambda_m} \frac{\lambda_s \rho_0^2 + \lambda_m B}{\rho_0^2}, \quad (56)$$

which increases as  $\rho_2$  increases. This implies that  $B_{c1}$  is a monotonically decreasing function with respect to  $\rho_1$ .

Moreover,  $Q_{out}$  is a monotonically increasing function of  $\sigma$  and  $\sigma$  increases as  $T$  increases, which implies that  $Q_{out}$  is a monotonically increasing function of  $\rho_1$ . Therefore, the outage-constrained feasible region of  $\rho_1$  becomes  $\rho_1 \in$

$$\eta_{ESE}(\rho_1, \rho_2; \lambda_m, \lambda_s, \lambda_u) = \frac{\lambda_m R_m \lambda_u + \lambda_s \rho_0^2 R_s \lambda_u}{B(\mathbf{P}_m(\rho_1, \rho_2; \lambda_m, \lambda_s, \lambda_u) + \mathbf{P}_s(\rho_1, \rho_2; \lambda_m, \lambda_s, \lambda_u))(\lambda_m + \lambda_s \rho_0^2)} \text{ [bit/Hz/Joule]}, \quad (43)$$

$$\mathbf{P}_m(\rho_1, \rho_2; \lambda_m, \lambda_s, \lambda_u) = \beta_m (\lambda_m + \lambda_s \rho_0^2) \left( \frac{p_{10} \mathcal{A}_0 + p_{11} \sum_{n'=1}^4 \mathcal{A}_{n'}}{(\alpha - 2)} \right) \left( \frac{K^K (\lambda_m + \lambda_s \rho_0^2)^K}{\left( K (\lambda_m + \lambda_s \rho_0^2) - \left( 2^{\frac{R_m}{B_{c1}}} - 1 \right) \lambda_u \right)^K} - 1 \right) + \lambda_m P_{OM}^m, \quad (44)$$

$$\mathbf{P}_s(\rho_1, \rho_2; \lambda_m, \lambda_s, \lambda_u) = \beta_s \left( \lambda_s + \frac{\lambda_m}{\rho_0^2} \right) \left( \frac{p_{20} \mathcal{B}_0 + p_{21} \sum_{n'=1}^4 \mathcal{B}_{n'}}{(\alpha - 2)} \right) \left( \frac{K^K \left( \lambda_s + \frac{\lambda_m}{\rho_0^2} \right)^K}{\left( K \left( \lambda_s + \frac{\lambda_m}{\rho_0^2} \right) - \left( 2^{\frac{R_s}{B_{c2}}} - 1 \right) \lambda_u \right)^K} - 1 \right) + \lambda_s P_{OS}^s. \quad (45)$$

$$\frac{\partial \mathbf{P}_m(\rho_1^*, \rho_2^*; \lambda_m, \lambda_s, \lambda_u)}{\partial \rho_1^*} + \frac{\partial \mathbf{P}_m(\rho_1^*, \rho_2^*; \lambda_m, \lambda_s, \lambda_u)}{\partial \rho_2^*} \frac{\partial \rho_2^*}{\partial \rho_1^*} + \frac{\partial \mathbf{P}_s(\rho_1^*, \rho_2^*; \lambda_m, \lambda_s, \lambda_u)}{\partial \rho_1^*} + \frac{\partial \mathbf{P}_s(\rho_1^*, \rho_2^*; \lambda_m, \lambda_s, \lambda_u)}{\partial \rho_2^*} \frac{\partial \rho_2^*}{\partial \rho_1^*} = 0 \quad (47)$$



$[\rho_0, Q_{out,1}^{-1}(\varepsilon_{out}; \lambda_m, \lambda_s, \lambda_u)]$ , where  $Q_{out,1}^{-1}(\cdot; \lambda_m, \lambda_s, \lambda_u)$  denotes the inverse function of  $Q_{out}(\rho_1, \rho_2; \lambda_m, \lambda_s, \lambda_u)$  with respect to the first argument  $\rho_1$ , and  $\rho_0 < Q_{out,1}^{-1}(\varepsilon_{out}; \lambda_m, \lambda_s, \lambda_u)$  always holds. Otherwise the BPwCo optimization (51) has no solution. From Proposition 7, we know that in the region of  $\rho_1 \in [\rho_0, \rho_1^*]$ ,  $\eta_{ESE}$  is a monotonically increasing function of  $\rho_1$ , and in the region of  $\rho_1 \in [\rho_1^*, +\infty)$ ,  $\eta_{ESE}$  is a monotonically decreasing function of  $\rho_1$ . Therefore, the outage-constrained optimal cross-tier inter-BS cooperation degree solution  $\rho_{1,out}^*$  of the BPwCo is given in the following straightforward theorem.

**Theorem 1:** Set  $Q_{out,1}^{-1}(\varepsilon_{out}^*; \lambda_m, \lambda_s, \lambda_u) = \rho_1^*$ . If  $Q_{out,1}^{-1}(\varepsilon_{out}; \lambda_m, \lambda_s, \lambda_u) < Q_{out,1}^{-1}(\varepsilon_{out}^*; \lambda_m, \lambda_s, \lambda_u) = \rho_1^*$ , i.e.,  $\varepsilon_{out} < \varepsilon_{out}^*$ , the outage-constrained cross-tier inter-BS cooperation degree solution is given by  $\rho_{1,out}^* = Q_{out,1}^{-1}(\varepsilon_{out}; \lambda_m, \lambda_s, \lambda_u)$ . If  $\varepsilon_{out} > \varepsilon_{out}^*$ , i.e.,  $Q_{out,1}^{-1}(\varepsilon_{out}; \lambda_m, \lambda_s, \lambda_u) > Q_{out,1}^{-1}(\varepsilon_{out}^*; \lambda_m, \lambda_s, \lambda_u) = \rho_1^*$ , the solution of the BPwCo (51) to (53) is given by  $\rho_{1,out}^* = \rho_1^*$ .

### B. Mobile-Traffic-Aware Joint Cross-Tier Inter-BS Cooperation and BS Deployment Optimization With Outage Constraint

In the case where a sufficient number of macro BSs are controllable by the network operator with a large number of small BSs switched on/off in the self-organized way, we can jointly optimize the cross-tier inter-BS cooperation factors  $\rho_1$  and  $\rho_2$  as well as macro and small BS densities  $\lambda_m$  and  $\lambda_s$  to maximize the network's ESE metric in a large-scale two-tier HCN for the given mobile-traffic intensity and average user rate, while satisfying all the users' QoS constraints.

Obviously, the ESE metric  $\eta_{ESE}$  is a function of the ratio  $\frac{\lambda_s}{\lambda_m}$ , and we also use  $\eta_{ESE}(\frac{\lambda_s}{\lambda_m})$  to reflect this relationship. The following straightforward proposition analyzes the unconstrained optimal macro/small BS density ratio solution that maximizes the network's ESE metric, given  $\rho_1, \rho_2$  and  $\lambda_u$ .

**Proposition 9:** There exists a unique optimal ratio of  $(\lambda_s/\lambda_m)^*$ , which maximizes the network's ESE metric  $\eta_{ESE}$  and it can be obtained numerically by solving

$$\frac{\partial \eta_{ESE}((\lambda_s/\lambda_m)^*)}{\partial (\lambda_s/\lambda_m)^*} = 0. \quad (57)$$

Noting (46), we will also denote the average cellular outage probability as  $Q_{out}(\rho_1; \lambda_s/\lambda_m, \lambda_u)$ . Combining both Propositions 8 and 9 leads to the following Proposition.

**Proposition 10:** There exists a unique globally optimal joint solution of the macro/small CoMP factor and the ratio of small/macro BS densities, denoted by  $(\rho_1^*, (\lambda_s/\lambda_m)^*)$ , which maximizes the network's ESE metric  $\eta_{ESE}$ , and can be numerically obtained by jointly solving the simultaneous equations of (47) and (57) with respect to  $\rho_1$  and  $\lambda_s/\lambda_m$ .

We finally introduce the outage-constrained, energy-spectral efficient and mobile-traffic-aware joint optimization of the macro/small CoMP factor and the small/macro BS density ratio, called JBwCoP for short. Specifically, given  $\lambda_u$ , the solution of the JBwCoP, denoted as  $(\rho_{1,out}^*, (\lambda_s/\lambda_m)_{out}^*)$ , is obtained by

solving the following optimization problem:

$$\left( \rho_{1,out}^*, \left( \frac{\lambda_s}{\lambda_m} \right)_{out}^* \right) = \arg \max_{\rho_1, \frac{\lambda_s}{\lambda_m}} \frac{\lambda_m R_m \lambda_u + \lambda_s \rho_0^2 R_s \lambda_u}{B(\mathbf{P}_m + \mathbf{P}_s) (\lambda_m + \lambda_s \rho_0^2)}, \quad (58)$$

$$\text{s.t. } \frac{\lambda_s}{\lambda_m} \in (Q_{out,2}^{-1}(\varepsilon_{out}; \rho_1; \lambda_u), +\infty), \quad (59)$$

$$\rho_1 \in (\rho_0, Q_{out,1}^{-1}(\varepsilon_{out}; \lambda_s/\lambda_m, \lambda_u)), \quad (60)$$

where  $Q_{out,2}^{-1}(\cdot; \rho_1; \lambda_u)$  in (59) is the inverse function of  $Q_{out}(\rho_1; \frac{\lambda_s}{\lambda_m}, \lambda_u)$  with respect to  $\frac{\lambda_s}{\lambda_m}$ , while (59) and (60) define the outage-constrained flexible regions for  $\rho_1$  and  $\frac{\lambda_s}{\lambda_m}$ , respectively. Note that (59) is obtained from the fact that  $Q_{out}(\rho_1; \frac{\lambda_s}{\lambda_m}, \lambda_u)$  is a monotonically decreasing function of  $\frac{\lambda_s}{\lambda_m}$ . By setting  $Q_{out}(\rho_1^*; (\frac{\lambda_s}{\lambda_m})_{out}^*, \lambda_u) = \varepsilon_{out}^*$ , the outage-constrained joint optimal solution of the JBwCoP,  $(\rho_{1,out}^*, (\frac{\lambda_s}{\lambda_m})_{out}^*)$ , is readily given in the following theorem.

**Theorem 2:** If  $\varepsilon_{out} > \varepsilon_{out}^*$  (Case 1), the outage-constrained optimal joint macro/small CoMP factor and the small/macro BS density ratio solution is given by  $(\rho_{1,out}^*, (\frac{\lambda_s}{\lambda_m})_{out}^*) = (\rho_1^*, (\frac{\lambda_s}{\lambda_m})^*)$ . If  $\varepsilon_{out} \leq \varepsilon_{out}^*$  (Case 2), the optimal joint solution is equivalent to finding the value of  $\rho_1$  that maximizes  $\eta_{ESE}$  in the region  $\rho_1 \in (\rho_0, Q_{out,1}^{-1}(\varepsilon_{out}; Q_{out,2}^{-1}(\varepsilon_{out}; \rho_1; \lambda_u), \lambda_u))$ .

**Remark 1:** In Case 1,  $(\rho_{1,out}^*, (\frac{\lambda_s}{\lambda_m})_{out}^*)$  is obviously located in the outage-constrained flexible region specified by (59) and (60). For Case 2, the unconstrained joint solution  $(\rho_1^*, (\frac{\lambda_s}{\lambda_m})^*)$  is not located within the outage-constrained flexible region. However, a set of outage-constrained joint optimal solutions can be obtained, which must satisfy the outage constraint  $Q_{out}(\rho_{1,out}; (\frac{\lambda_s}{\lambda_m})_{out}, \lambda_u) = \varepsilon_{out}$ . Hence, by using  $\frac{\lambda_s}{\lambda_m} = Q_{out,2}^{-1}(\varepsilon_{out}; \rho_1; \lambda_u)$ , we can obtain the solution of Case 2. Note that this one-variable optimization can be solved efficiently using, for example, the binary search algorithm [25].

### C. Limitations, Implementation and Future Extension

In our derivation, we assume that both the UE and BS are equipped with a single antenna. This is a limitation of our proposed design, which will be addressed in our future research, since our cellular networks have increasingly become MIMO based. However, the proposed system model is based on solid theoretical and practical foundations, and the implementation of our proposed ESE optimization framework for large-scale CoMP-aided HCNs to real-world (single-antenna) systems is straightforward. To the best of our knowledge, there is no existing work on mobile-traffic-aware joint CoMP and BS deployment strategy that maximizes the global ESE for large-scale CoMP-aided HCNs relying on MIMO techniques. Hence extending the proposed framework to MIMO aided networks is an important future piece of work.

This also naturally leads to the concept of cell-free massive MIMO communication networks [26], [27], [28], which is an on-going extension of our communication networks to the next generation systems. The cell-free concept is a natural extension of CoMP to the limit. In a cell-free system, there exists no cell

TABLE III  
BASIC SYSTEM PARAMETERS

System Parameter	Value
$\alpha$	2.5~4
$P_m, P_s$	20 W, 1 W
$\varepsilon_{out}$	0.2
$\beta_m, \beta_s$	1.0, 1.0
$B$	15~25 MHz
$R_m, R_s$	0.1~0.35 Mbit/s
$P_{OM}^m, P_{OM}^s$	20 W, 0.5 W

boundary, and all the access points (APs) work collaboratively to support every user. Such a cell-free communication network is necessarily based on the massive MIMO concept. Extensive research efforts have been focused on cell-free massive MIMO communication networks, including their performance analysis based on the stochastic geometry based approach [26]. However, no study has considered the mobile-traffic-aware AP deployment strategy that maximizes the global ESE for cell-free massive MIMO communication networks, which is an extremely challenging task and it will be our long-term research goal.

## V. NUMERICAL AND SIMULATION RESULTS

In this section, the numerical and simulation results are discussed, where the ESE metric for the large-scale two-tier HCN with the cross-tier inter-BS cooperation enhancement is portrayed in various practical circumstances and its accuracy is correspondingly verified. Moreover, the resource saving ratio (RSR) is adopted to quantify the gain of our optimized design strategies, which can be expressed as

$$RSR = \frac{ARC_{base} - ARC_{opt}}{ARC_{base}}, \quad (61)$$

where  $ARC_{base}$  and  $ARC_{opt}$  denotes the area resource consumptions required by the existing state-of-the-art baseline design of [8], [17], [19], [29], [30] and our proposed optimized design, respectively. The basic system parameters are given in Table III.

### A. Key System Performance Indicators

Fig. 1 depicts the network's ESE as the function of the CoMP factor  $\frac{\rho_1}{\rho_0}$  and the ratio of small BS density to macro BS density  $\frac{\lambda_s}{\lambda_m}$ , given the bandwidth resource  $B = 15$  MHz, the average user rate  $R_m = R_s = 0.15$  Mbits/s, the UE density  $\lambda_u = 600$  UE/km<sup>2</sup>, the pathloss exponent  $\alpha = 2.5$  and the inter-tier weight factor  $\mu = 10$ . It can be seen from Fig. 1 that, given  $\frac{\lambda_s}{\lambda_m}$ , there exists a unique point  $\rho_1^*/\rho_0$  that maximizes the network's ESE, which validates Proposition 7. Similarly, given  $\rho_1/\rho_0$ , there exists a unique  $(\lambda_s/\lambda_m)^*$  that maximizes the ESE, as proved in Proposition 9. More significantly, there exists a unique globally optimal joint solution of the CoMP factor and the ratio of small and macro BS densities  $(\rho_1^*/\rho_0, (\lambda_s/\lambda_m)^*)$  that maximizes the network's ESE, which validates Proposition 10. It can also be seen from Fig. 1 that the CoMP factor  $\rho_1/\rho_0$  has some impact on the optimal  $(\lambda_s/\lambda_m)^*$ . On the other hand, increasing  $\lambda_s/\lambda_m$  leads to the decrease of the optimal  $\rho_1^*/\rho_0$ ,

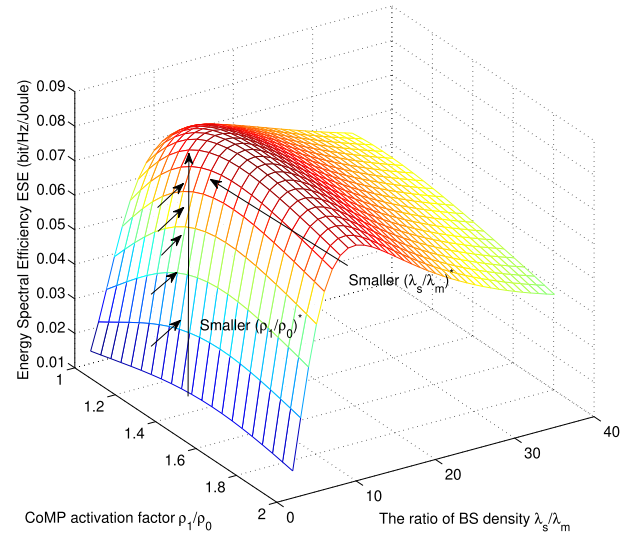


Fig. 1. Network' ESE as the function of CoMP factor  $\rho_1/\rho_0$  and ratio of small BS density to macro BS density  $\lambda_s/\lambda_m$ , given bandwidth resource  $B = 15$  MHz, average user rate  $R_m = R_s = 0.15$  Mbits/s, UE density  $\lambda_u = 600$  UE/km<sup>2</sup>, pathloss exponent  $\alpha = 2.5$  and inter-tier weight factor  $\mu = 10$ .

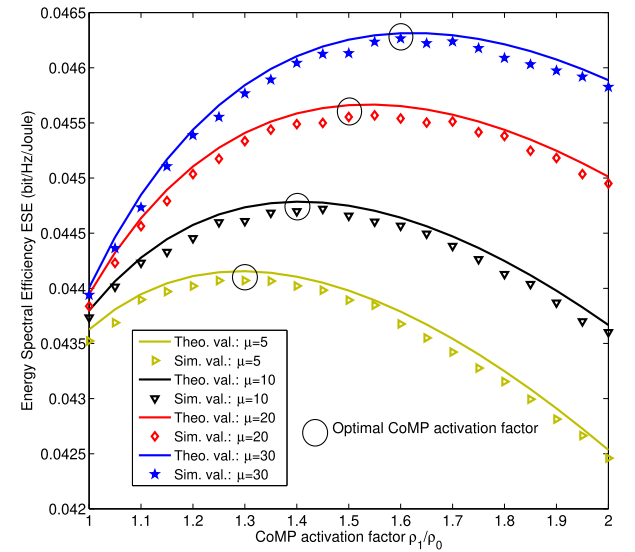


Fig. 2. Theoretical and simulated network's ESEs versus CoMP factor  $\rho_1/\rho_0$  for different  $\mu$ , given  $B = 20$  MHz,  $\lambda_m = 5$  BS/km<sup>2</sup>,  $\lambda_s = 200$  BS/km<sup>2</sup>,  $\lambda_u = 600$  UE/km<sup>2</sup>,  $R_m = R_s = 0.15$  Mbits/s and  $\alpha = 4$ .

which implies that we have to enable more UE to operate into cross-tier CoMP mode to maximize the network's ESE when the small BS density is low, and vice versa. In other words, the ESE performance gain resulted from cross-tier inter-BS cooperation can be replaced by denser small BS deployment.

The theoretical and simulated network's ESEs versus the CoMP factor  $\rho_1/\rho_0$  for different  $\mu$  are depicted in Fig. 2, given  $B = 20$  MHz,  $\lambda_m = 5$  BS/km<sup>2</sup>,  $\lambda_s = 200$  BS/km<sup>2</sup>,  $\lambda_u = 600$  UE/km<sup>2</sup>,  $R_m = R_s = 0.15$  Mbits/s and  $\alpha = 4$ . It can be seen that the theoretical values agree well with the simulation results, which validates our theoretical analysis. Also observe from

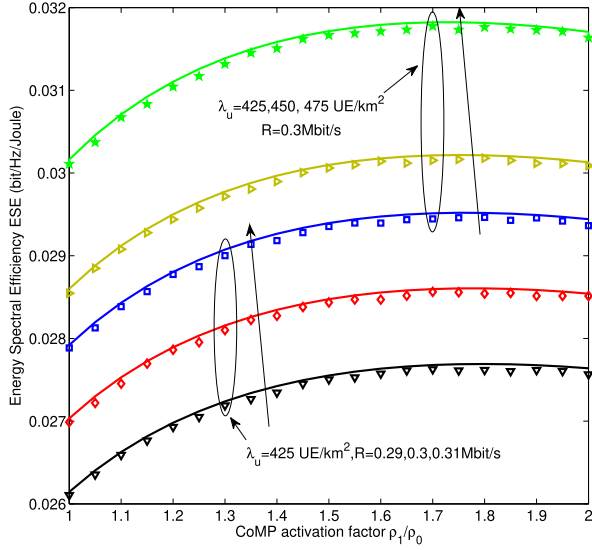


Fig. 3. Theoretical and simulated network's ESEs versus CoMP factor  $\rho_1/\rho_0$  for different  $\lambda_u$  and  $R_m = R_s = R$ , given  $B = 20$  MHz,  $\lambda_m = 6$  BS/km<sup>2</sup>,  $\lambda_s = 225$  BS/m<sup>2</sup>,  $\mu = 10$  and  $\alpha = 4$ .

Fig. 2 that the higher  $\mu$  is, the more UE have to be involved in cross-tier inter-BS cooperation in line with increasing  $\rho_1/\rho_0$  to maximize the network's ESE. The reason behind it is that increasing  $\mu$  can reduce the small cells' coverage area while increasing the coverage area of macro cells. The effort of this is twofold. First, this enables some small UE to seek CoMP association with macro BSs. Second, portion of macro UE are close to the interference from small-tier and have high CoMP demands. Both contribute to the increase of the optimal  $\rho_1^*/\rho_0$ . Thus the increase of  $\mu$  can obtain a higher ESE performance by cross-tier CoMP.

Fig. 3 portrays the network's ESE as the function of the CoMP factor  $\rho_1/\rho_0$  for different  $\lambda_u$  and  $R = R_m = R_s$ , given  $B = 20$  MHz,  $\lambda_m = 6$  BS/km<sup>2</sup>,  $\lambda_s = 225$  BS/km<sup>2</sup>,  $\mu = 10$  and  $\alpha = 4$ . Obviously, more ESE benefits can be obtained by cross-tier CoMP when the average user rate or the UE density is increased with more DL transmit power been consumed. However, different with the impact of  $\mu$  on the ESE shown in Fig. 2, the change in  $\lambda_u$  or  $R$  does not alter the gradient of the ESE with respect to  $\rho_1/\rho_0$  much.

Fig. 4 depicts the network's ESE as the function of the CoMP factor  $\rho_1/\rho_0$  for different  $B$  and  $\alpha$ , given  $R_m = R_s = 0.15$  Mbits/s,  $\lambda_m = 5$  BS/km<sup>2</sup>,  $\lambda_s = 200$  BS/km<sup>2</sup>,  $\lambda_u = 500$  UE/km<sup>2</sup> and  $\mu = 20$ . Given the bandwidth  $B$ , increasing  $\alpha$  increases the achievable ESE as well as reduces the ESE's sensitivity with respect to  $\rho_1/\rho_0$ . This indicates that low channel quality can increase the UE's CoMP demand and high channel quality is beneficial to the ESE performance benefits. By contrast, given the pathloss exponent  $\alpha$ , increasing  $B$  does not seem to influence the ESE's sensitivity with respect to  $\rho_1/\rho_0$  and the location of the maximum ESE, but decreases the achievable ESE since wider bandwidth can reduce UE's power consumption.

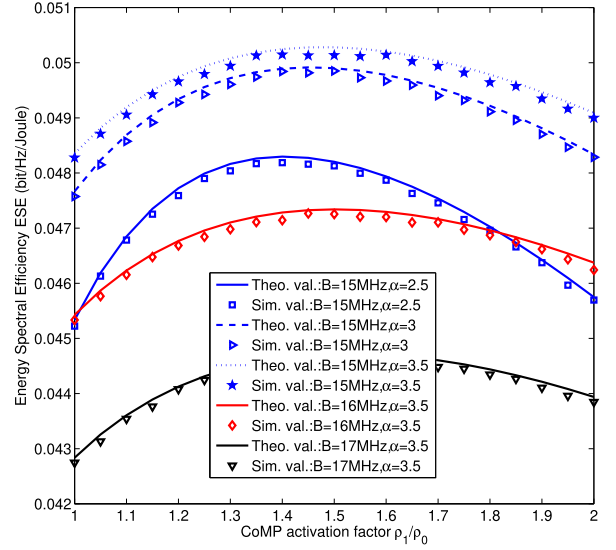


Fig. 4. Theoretical and simulated network's ESEs versus CoMP factor  $\rho_1/\rho_0$  for different  $B$  and  $\alpha$ , given  $R_m = R_s = 0.2$  Mbits/s,  $\lambda_m = 5$  BS/km<sup>2</sup>,  $\lambda_s = 200$  BS/km<sup>2</sup>,  $\lambda_u = 500$  UE/km<sup>2</sup> and  $\mu = 20$ .

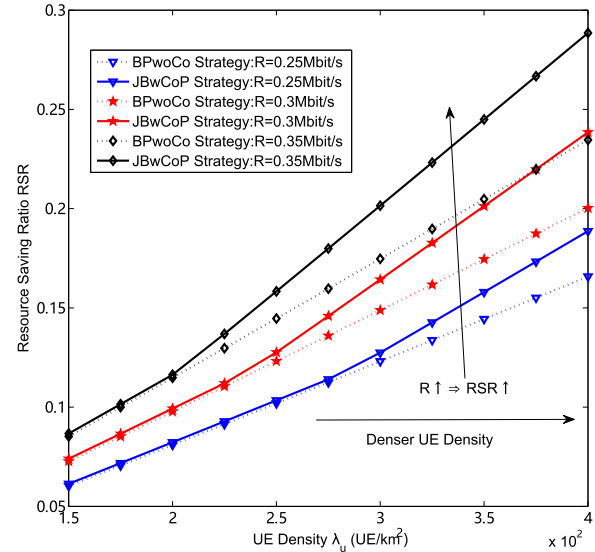


Fig. 5. RSRs achieved by our BPwCo and JBwCoP as the functions of the network's UE density  $\lambda_u$  for different  $R_m = R_s = R$ , given macro BS density  $\lambda_m = 5$  BS/km<sup>2</sup>, small BS density  $\lambda_s = 10$  BS/km<sup>2</sup>, bandwidth  $B = 20$  MHz, pathloss exponent  $\alpha = 4$  and inter-tier weight factor  $\mu = 20$ .

## B. Evaluation of RSR

We now evaluate the RSRs achieved by our proposed two design strategies, BPwCo and JBwCoP, in typical CoMP-enhanced two-tier HetNet scenarios. Recall from (61) that the RSR is the normalized area resource consumption saving achieved by our optimization design over the baseline design of [19], [29], [30]. First, Fig. 5 shows the RSRs achieved by our BPwCo and JBwCoP as the functions of the network's UE density  $\lambda_u$  for different average user rates  $R_m = R_s = R$ ,

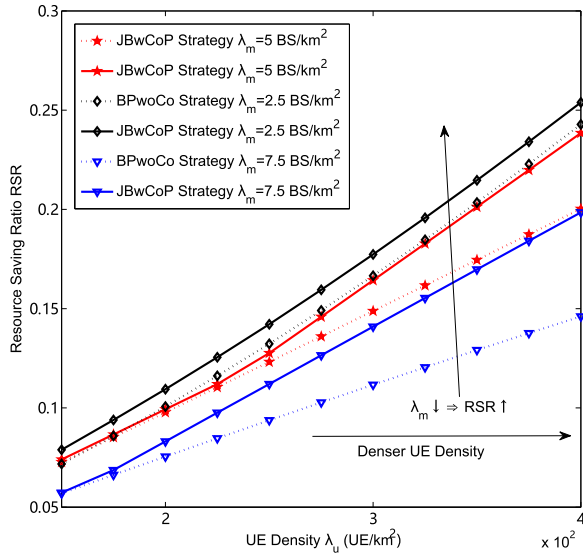


Fig. 6. RSRs achieved by the proposed BPwCo and JBwCoP as the functions of UE density  $\lambda_u$  for different  $\lambda_m$ , given  $\lambda_s = 10$  BS/km<sup>2</sup>,  $B = 20$  MHz,  $R_m = R_s = R = 0.35$  Mbits/s,  $\alpha = 4$  and  $\mu = 20$ .

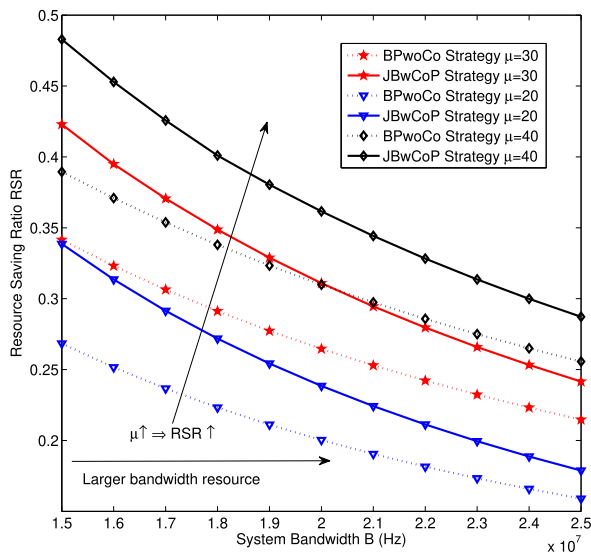


Fig. 7. RSRs achieved by the proposed BPwCo and JBwCoP as the functions of bandwidth resource  $B$  for different  $\mu$ , given  $\lambda_m = 5$  BS/km<sup>2</sup>,  $\lambda_s = 10$  BS/km<sup>2</sup>,  $\lambda_u = 400$  UE/km<sup>2</sup>,  $R_m = R_s = 0.35$  Mbits/s,  $\alpha = 4$  and  $\mu = 20$ .

given the macro BS density  $\lambda_m = 5$  BS/km<sup>2</sup>, the small BS density  $\lambda_s = 10$  BS/km<sup>2</sup>, the bandwidth resource  $B = 20$  MHz, the pathloss exponent  $\alpha = 4$  and the inter-tier weight factor  $\mu = 20$ . It can be seen from Fig. 5 that the achievable RSR performance of our two proposed strategies increase as the UE density  $\lambda_u$  or the average user rate  $R$  increases. It can also be observed that the JBwCoP strategy performs better than the BPwCo strategy, in terms of RSR, particularly when  $\lambda_u$  is sufficiently high. Moreover, the performance gap between the two optimization strategies increases with  $R$ .

Next Fig. 6 depicts the RSRs achieved by the proposed BPwCo and JBwCoP as the functions of the network's UE density

$\lambda_u$  for different macro BS densities  $\lambda_m$ , given  $\lambda_s = 10$  BS/km<sup>2</sup>,  $B = 20$  MHz,  $R_m = R_s = R = 0.35$  Mbits/s,  $\alpha = 4$  and  $\mu = 20$ . It can be seen that increasing  $\lambda_u$  improves the achievable RSR while increasing  $\lambda_m$  degrades the achievable RSR for our both designs. More importantly, the JBwCoP strategy clearly outperforms the BPwCo design, in terms of RSR.

Then in Fig. 7, we illustrate the RSRs achieved by the proposed BPwCo and JBwCoP with respect to the bandwidth resource  $B$  for different inter-tier weight factors  $\mu$ , given  $\lambda_m = 5$  BS/km<sup>2</sup>,  $\lambda_s = 10$  BS/km<sup>2</sup>,  $\lambda_u = 400$  UE/km<sup>2</sup>,  $R_m = R_s = 0.35$  Mbits/s,  $\alpha = 4$  and  $\mu = 20$ . It can be seen that the achievable RSRs of our both designs decrease with the increase in the bandwidth resource  $B$ , while the RSRs of our both strategies increase with the increase of the inter-tier weight factor  $\mu$ . Again observe that the proposed JBwCoP design significantly outperforms the proposed BPwCo design, in terms of RSR, which again confirms the effectiveness of the joint optimization strategy of JBwCoP.

## VI. CONCLUSION

The energy-spectral efficiency of the large-scale CoMP-enhanced two-tier HCNs has been modeled. In particular, an accurate network ESE expression has been derived as a function of the key cellular parameters, including the macro- and small-cell CoMP activation factors, the macro- and small-cell BS densities, the UE density, the system bandwidth and the average data rate requirement. We have carried out the joint analysis of CoMP and BS deployment by specifically considering the impact of the network's UE density and other key cellular parameters on the network's ESE. Most significantly, we have designed a pair of optimization strategies for maximizing the network's ESE metric. The first design is based on cellular-scenario-aware CoMP optimization under specific outage constraints, while the second design performs mobile-traffic-aware joint CoMP and BS deployment optimization under an outage probability constraint. Our theoretical analysis and simulation results have demonstrated that the required system resources can be significantly reduced by our design strategies. Not surprisingly, the joint CoMP and BS deployment optimization design has been shown to be particularly effective in conserving system resources. Our study thus has offered valuable insights and guidelines for network operators concerning the benefits of CoMP and BS deployment techniques in dense large-scale HCNs.

Our future research may extend the results to large-scale CoMP-aided two-tier HCNs where more than two cross-tier BSs collaborate. The theoretical model conceived may be beneficially used by network operators for characterizing the complex interplay between the network performance and the key factors influencing it. In addition, further research efforts are required to extend our design to MIMO based large-scale CoMP-aided HCNs, and our long-term research goal will be to design efficient mobile-traffic-aware AP deployment strategy that maximizes the global ESE for cell-free massive MIMO networks.

## APPENDIX

## A. Proof of Lemma 1

*Proof:* Since  $\Psi_m$  and  $\Psi_s$  follow two independent PPPs, the joint probability density function (p.d.f.) of  $r_0$  (3) and  $r_1$  (4) is given by  $f_{r_0, r_1} = f_{r_0} \cdot f_{r_1}$ , where the p.d.f.s of  $r_0$  and  $r_1$  are given respectively by [3]

$$f_{r_0} = 2\pi\lambda_m r_0 \exp(-\pi\lambda_m r_0^2), \quad (62)$$

$$f_{r_1} = 2\pi\lambda_s r_1 \exp(-\pi\lambda_s r_1^2). \quad (63)$$

The No-CoMP probability for a typical macro UE  $u_{m_i}$  with  $r_1 \geq r_0\rho_1$  is given by

$$p_{10} = \int_0^{+\infty} \int_{r_0\rho_1}^{+\infty} f_{r_0} \cdot f_{r_1} dr_1 dr_0, \quad (64)$$

which leads to (8) (see, for example, [12], [18]). Similarly, the CoMP probability for a typical macro UE  $u_{m_i}$  with  $r_0\rho_0 \leq r_1 \leq r_0\rho_1$  is given by

$$p_{11} = \int_0^{+\infty} \int_{r_0\rho_0}^{r_0\rho_1} f_{r_0} \cdot f_{r_1} dr_1 dr_0. \quad (65)$$

This results in (7). Likewise, the No-CoMP probability for a typical small UE  $u_{s_j}$  with  $\bar{r}_1/\rho_2 \leq \bar{r}_0$  is given by

$$p_{20} = \int_0^{+\infty} \int_{\bar{r}_1/\rho_2}^{+\infty} f_{\bar{r}_0} \cdot f_{\bar{r}_1} d\bar{r}_0 d\bar{r}_1, \quad (66)$$

which leads to (10), and the CoMP probability for a typical small UE  $u_{s_j}$  with  $\bar{r}_1/\rho_0 \leq \bar{r}_0 \leq \bar{r}_1/\rho_2$  is given by

$$p_{21} = \int_0^{+\infty} \int_{\bar{r}_1/\rho_0}^{\bar{r}_1/\rho_2} f_{\bar{r}_0} \cdot f_{\bar{r}_1} d\bar{r}_0 d\bar{r}_1, \quad (67)$$

which results in (9). This completes the proof.  $\blacksquare$

## B. Proof of Proposition 1

*Proof:* The average DL transmit power from macro BS  $m_i$  to the  $k'$ -th No-CoMP macro UE  $u_{m_i}^{k'}$  associated with the subband  $B_{k'}$  of the interior-resources  $B_{c1}$  conditioned on  $r_0$ ,  $r_1$  and the interference layout  $\{\Psi_m \cup \Psi_s\} \setminus m_i$  is given by

$$\begin{aligned} E [P_{k'}^{Tx} | r_0, r_1, \{\Psi_m \cup \Psi_s\} \setminus m_i] &= E \left[ \left( 2^{\frac{R_{k'}}{B_{k'}}} - 1 \right) \frac{r_0^\alpha}{h_{k'}^i} I_{k'} \right] \\ &= E \left[ \left( 2^{\frac{R_{k'}}{B_{k'}}} - 1 \right) r_0^\alpha \frac{\partial}{\partial s} \ln (\mathcal{M}_{I_{k'}}(s)) \Big|_{s=0} \right], \end{aligned} \quad (68)$$

where  $\mathcal{M}_{I_{k'}}(s)$  denotes the moment generating function (MGF) of  $I_{k'}$ , the first equality is obtained by applying the rate formula  $R_{k'}$  (11), while the second equality is based on the well-known property of MGF and  $E[h_{k'}^i] = 1$ . The MGF  $\mathcal{M}_{I_{k'}}(s)$  can be obtained from [31], and the average DL transmit power conditioned on  $r_0$  and  $r_1$  becomes (see, for example, [2], [18])

$$\begin{aligned} E [P_{k'}^{Tx} | r_0, r_1] &= \left( 2^{\frac{R_{k'}}{B_{k'}}} - 1 \right) \frac{2\pi B_{k'} r_0^2}{(\alpha - 2) B_{c1}} \\ &\quad \times (\lambda_m P_{\text{In}}^m + \lambda_s P_{\text{In}}^s \rho_1^{2-\alpha}). \end{aligned} \quad (69)$$

Adopting the p.d.f.s of  $r_0$  and  $r_1$  gives rise to

$$E [P_{k'}^{Tx}] = \int_0^{+\infty} \int_{r_0\rho_1}^{+\infty} f_{r_0, r_1} E [P_{k'}^{Tx} | r_0, r_1] dr_1 dr_0. \quad (70)$$

Completing the integration in (70) by noting  $P_m = N_i P_{\text{In}}^m$  and  $P_s = N_j P_{\text{In}}^s$  leads to (23).  $\blacksquare$

## C. Proof of Proposition 2

*Proof:* The average DL transmit power of typical macro CoMP UE  $u_{m_i}^k$  requiring the service rate of  $R_k$  as well as associated with the interior subband  $B_k$  of  $B_{c1}$  in macro-BS  $m_i$  and the outer subband  $B_k$  of  $B_{c2}^{\text{Out}}$  in small BS  $s_k^{CT}$ , conditioned on  $r_0$ ,  $r_1$  and interferer set  $\{\Psi_m \cup \Psi_s\} \setminus (m_i, s_k^{CT})$ , can be expressed as

$$\begin{aligned} E [P_{k,1}^{Tx} + P_{k,2}^{Tx} | r_0, r_1, \{\Psi_m \cup \Psi_s\} \setminus (m_i, s_k^{CT})] \\ &= E \left[ \left( 2^{\frac{R_k}{B_k}} - 1 \right) \left( \frac{r_0^\alpha}{2h_k^i} + \frac{r_1^\alpha}{2h_k^{CT}} \right) I_k \right] \\ &= E \left[ \left( 2^{\frac{R_k}{B_k}} - 1 \right) \frac{r_0^\alpha}{2} \frac{\partial}{\partial s} \ln (\mathcal{M}_{I_k}(s)) \Big|_{s=0} \right] \\ &\quad + E \left[ \left( 2^{\frac{R_k}{B_k}} - 1 \right) \frac{r_1^\alpha}{2} \frac{\partial}{\partial s} \ln (\mathcal{M}_{I_k}(s)) \Big|_{s=0} \right]. \end{aligned} \quad (71)$$

The first equality is obtained by applying the rate formula  $R_k$  of (13) in conjunction with  $P_{k,1}^{Tx} L_k^i h_k^i = P_{k,2}^{Tx} L_k^{CT} h_k^{CT}$ , while the second equality is based on the well-known property of MGF as well as  $E[h_k^i] = E[h_k^{CT}] = 1$ . Similar to Appendix B, after calculating  $\mathcal{M}_{I_k}(s)$  according to [31], we obtain the total average DL transmit power to  $u_{m_i}^k$  conditioned on  $r_0$  and  $r_1$  as follows:

$$\begin{aligned} E [P_k^{Tx} | r_0, r_1] &= \frac{\pi (2^{R_k/B_k} - 1) B_k}{(\alpha - 2) B_{c1}} (\lambda_m P_{\text{In}}^m r_0^2 \\ &\quad + \lambda_s P_{\text{In}}^s r_1^{2-\alpha} r_0^\alpha + \lambda_m P_{\text{In}}^m r_0^{2-\alpha} r_1^\alpha \\ &\quad + \lambda_s P_{\text{In}}^s r_1^2). \end{aligned} \quad (72)$$

Furthermore, applying the p.d.f.s of  $r_0$  and  $r_1$  leads to

$$E [P_k^{Tx}] = \frac{(2^{R_k/B_k} - 1) (\lambda_m + \lambda_s \rho_0^2)}{(\alpha - 2) \lambda_u} \sum_{n'=1}^4 \mathcal{A}_{n'}, \quad (73)$$

where

$$\mathcal{A}_1 = \int_0^{+\infty} \int_{r_0\rho_0}^{r_0\rho_1} \pi \lambda_m P_{\text{In}}^m r_0^2 f_{r_0, r_1} dr_1 dr_0, \quad (74)$$

$$\mathcal{A}_2 = \int_0^{+\infty} \int_{r_0\rho_0}^{r_0\rho_1} \pi \lambda_s P_{\text{In}}^s r_1^{2-\alpha} r_0^\alpha f_{r_0, r_1} dr_1 dr_0, \quad (75)$$

$$\mathcal{A}_3 = \int_0^{+\infty} \int_{r_0\rho_0}^{r_0\rho_1} \pi \lambda_m P_{\text{In}}^m r_0^{2-\alpha} r_1^\alpha f_{r_0, r_1} dr_1 dr_0, \quad (76)$$

$$\mathcal{A}_4 = \int_0^{+\infty} \int_{r_0\rho_0}^{r_0\rho_1} \pi \lambda_s P_{\text{In}}^s r_1^2 f_{r_0, r_1} dr_1 dr_0. \quad (77)$$

Completing the integrations in (74)–(77) leads to (25)–(28).  $\blacksquare$

#### D. Proof of Proposition 3

*Proof:* The average DL transmit power of small BS  $s_j$  to typical No-CoMP small UE  $u_{s_j}^l$  requiring service rate  $R_l$  and associated with the interior subband  $B_l$  of  $B_{c2}$ , conditioned on  $r_0, r_1$  and the interferer set  $\{\Psi_m \cup \Psi_s\} \setminus s_j$ , is given by

$$\begin{aligned} E [P_l^{Tx} | r_0, r_1, \{\Psi_m \cup \Psi_s\} \setminus s_j] &= E \left[ \left( 2^{\frac{R_l}{B_l}} - 1 \right) \frac{r_1^\alpha}{h_l^\alpha} I_l \right] \\ &= E \left[ \left( 2^{\frac{R_l}{B_l}} - 1 \right) r_1^\alpha \frac{\partial}{\partial s} \ln (\mathcal{M}_{I_l}(s)) \Big|_{s=0} \right]. \end{aligned} \quad (78)$$

Similar to the proofs of Propositions 1 and 2, we have

$$\begin{aligned} E [P_l^{Tx} | r_0, r_1] &= \left( 2^{\frac{R_l}{B_l}} - 1 \right) \frac{2\pi B_l}{(\alpha - 2)B_{c2}} \\ &\quad \times (\lambda_s P_{\text{In}}^s + \lambda_m P_{\text{In}}^m \rho_2^{2-\alpha}) r_1^2. \end{aligned} \quad (79)$$

Therefore, the average DL transmit power is given by

$$E [P_l^{Tx}] = \int_0^{+\infty} \int_{r_1/\rho_2}^{+\infty} f_{r_0, r_1} E [P_l^{Tx} | r_0, r_1] dr_0 dr_1. \quad (80)$$

Carrying out the integration in (80) leads to (31). ■

#### E. Proof of Proposition 4

*Proof:* The average total DL transmit power for typical small CoMP UE  $u_{s_j}^l$  requiring service rate  $R_l$ , associated with the interior subband  $B_l$  of  $B_{c2}$  in small-BS  $s_j$  and the outer subband  $B_l$  of  $B_{c1}^{\text{out}}$  in macro BS  $m_l^{CT}$ , conditioned on  $r_0, r_1$  and the interferer set  $\{\Psi_m \cup \Psi_s\} \setminus (s_j, m_l^{CT})$ , is given by

$$\begin{aligned} E [P_{l,1}^{Tx} + P_{l,2}^{Tx} | r_0, r_1, \{\Psi_m \cup \Psi_s\} \setminus (s_j, m_l^{CT})] \\ &= E \left[ \left( 2^{\frac{R_l}{B_l}} - 1 \right) \frac{r_0^\alpha}{2} \frac{\partial}{\partial s} \ln (\mathcal{M}_{I_l}(s)) \Big|_{s=0} \right] \\ &\quad + E \left[ \left( 2^{\frac{R_l}{B_l}} - 1 \right) \frac{r_1^\alpha}{2} \frac{\partial}{\partial s} \ln (\mathcal{M}_{I_l}(s)) \Big|_{s=0} \right]. \end{aligned} \quad (81)$$

Similar to Appendix C, we obtain the total average DL transmit power for  $u_{s_j}^l$ , conditioned on  $r_0$  and  $r_1$ , as

$$\begin{aligned} E [P_l^{Tx} | r_0, r_1] &= \frac{\pi (2^{R_l/B_l} - 1) B_l}{(\alpha - 2)B_{c1}} (\lambda_s P_{\text{In}}^s r_1^2 \\ &\quad + \lambda_m P_{\text{In}}^m r_0^{2-\alpha} r_1^\alpha + \lambda_s P_{\text{In}}^s r_1^{2-\alpha} r_0^\alpha \\ &\quad + \lambda_m P_{\text{In}}^m r_0^2). \end{aligned} \quad (82)$$

Therefore, by deconditioning on  $r_0$  and  $r_1$ , we have

$$E [P_l^{Tx}] = \frac{(2^{R_l/B_l} - 1)}{\lambda_u (\alpha - 2)} \left( \lambda_s + \frac{\lambda_m}{\rho_0^2} \right) \sum_{n'=1}^4 \mathcal{B}_{n'}, \quad (83)$$

where

$$\mathcal{B}_1 = \int_0^{+\infty} \int_{r_1/\rho_0}^{r_1/\rho_2} \pi \lambda_s P_{\text{In}}^s r_1^2 f_{r_0, r_1} dr_0 dr_1, \quad (84)$$

$$\mathcal{B}_2 = \int_0^{+\infty} \int_{r_1/\rho_0}^{r_1/\rho_2} \pi \lambda_m P_{\text{In}}^m r_0^{2-\alpha} r_1^\alpha f_{r_0, r_1} dr_0 dr_1, \quad (85)$$

$$\mathcal{B}_3 = \int_0^{+\infty} \int_{r_1/\rho_0}^{r_1/\rho_2} \pi \lambda_s P_{\text{In}}^s r_1^{2-\alpha} r_0^\alpha f_{r_0, r_1} dr_0 dr_1, \quad (86)$$

$$\mathcal{B}_4 = \int_0^{+\infty} \int_{r_1/\rho_0}^{r_1/\rho_2} \pi \lambda_m P_{\text{In}}^m r_0^2 f_{r_0, r_1} dr_0 dr_1. \quad (87)$$

Like in Appendix C, carrying out the integrations in (84)–(87) leads to (33)–(36). ■

#### F. Proof of Proposition 5

*Proof:* For macro BS  $m_i$  serving  $N_i$  UEs and having cell coverage area  $A_m$ , the probability mass function (PMF) of  $N_i$  is given by  $F_{A_m}(N_i) = (\lambda_u A_m)^{N_i} \exp(-\lambda_u A_m) / N_i!$  with  $N_i \geq 0$  [31]. Based on Propositions 1 and 2, the averaged aggregate DL transmit power of typical macro-cell  $V_{m_i}$  conditioned on  $A_m$  can be expressed as

$$\begin{aligned} E [P_m^{Tx} | A_m] \\ &= E_{N_i} \left[ \sum_k E [P_k^{Tx} | N_i] + \sum_{k'} E [P_{k'}^{Tx} | N_i] \right] \\ &= \frac{\mathcal{C}_1}{(\alpha - 2)} \sum_{N_i=1}^{\infty} \frac{\left( 2^{\frac{N_i R_m}{B_{c1}}} - 1 \right) (\lambda_u A_m)^{N_i}}{N_i!} \exp(-\lambda_u A_m) \\ &= \frac{\mathcal{C}_1}{(\alpha - 2)} \sum_{N_i=0}^{\infty} \left( 2^{\frac{N_i R_m}{B_{c1}}} \frac{(\lambda_u A_m)^{N_i}}{N_i!} - 1 \right) \exp(-\lambda_u A_m) \\ &\quad - \frac{\mathcal{C}_1}{(\alpha - 2)} \sum_{N_i=0}^{\infty} \left( \frac{(\lambda_u A_m)^{N_i}}{N_i!} - 1 \right) \exp(-\lambda_u A_m) \\ &= \frac{\mathcal{C}_1}{(\alpha - 2)} \left( \exp \left( \left( 2^{\frac{R_m}{B_{c1}}} - 1 \right) \lambda_u A_m \right) - 1 \right), \end{aligned} \quad (88)$$

where  $\mathcal{C}_1 = (p_{10} \mathcal{A}_0 + p_{11} \sum_{n'=1}^4 \mathcal{A}_{n'}) / (p_{10} + p_{11})$ .

According to [32], an approximate p.d.f. of  $A_m$  is  $f(A_m) = K^K (\lambda_m + \lambda_s \rho_0^2)^K A_m^{K-1} \exp(-K(\lambda_m + \lambda_s \rho_0^2) A_m) / \Gamma(K)$ , where  $K = 3.75$  and  $\Gamma(x) = \int_0^{+\infty} t^{x-1} \exp(-t) dt$ . By using this p.d.f. with (88), the average DL aggregate transmit power for typical macro cell  $V_{m_i}$  is given by

$$\begin{aligned} E [P_m^{TX}] &= \frac{\mathcal{C}_1}{(\alpha - 2)} \left( \int_0^{+\infty} (\lambda_m + \lambda_s \rho_0^2)^K \right. \\ &\quad \times \exp(-K(\lambda_m + \lambda_s \rho_0^2) A_m) \frac{K^K A_m^{K-1}}{\Gamma(K)} \\ &\quad \times \exp \left( \left( 2^{\frac{R_m}{B_{c1}}} - 1 \right) \lambda_u A_m \right) dA_m - 1 \Big). \end{aligned} \quad (89)$$

Carrying out the integration in (89) leads to (39).

In a similar way, we can also obtain the averaged aggregate small DL transmit power for typical small BS of (40). ■

## REFERENCES

- [1] C.-L. I, C. Rowell, S. Han, Z. Xu, G. Li, and Z. Pan, "Toward green and soft: A 5G perspective," *IEEE Commun. Mag.*, vol. 52, no. 2, pp. 66–73, Feb. 2014.
- [2] G. Zhao, S. Chen, L. Zhao, and L. Hanzo, "A tele-traffic-aware optimal base-station deployment strategy for energy-efficient large-scale cellular networks," *IEEE Access*, vol. 4, pp. 2083–2095, 2016.
- [3] J. G. Andrews, F. Baccelli, and R. K. Ganti, "A tractable approach to coverage and rate in cellular networks," *IEEE Trans. Commun.*, vol. 59, no. 11, pp. 3122–3134, Nov. 2011.
- [4] H. Zhang, S. Chen, L. Feng, Y. Xie, and L. Hanzo, "A universal approach to coverage probability and throughput analysis for cellular networks," *IEEE Trans. Veh. Technol.*, vol. 64, no. 9, pp. 4245–4256, Sep. 2015.
- [5] H. S. Dhillon, R. K. Ganti, F. Baccelli, and J. G. Andrews, "Modeling and analysis of K-tier downlink heterogeneous cellular networks," *IEEE J. Sel. Areas Commun.*, vol. 30, no. 3, pp. 550–560, Apr. 2012.
- [6] M. D. Renzo, A. Zappone, T. T. Lam, and M. Debbah, "System-level modeling and optimization of the energy efficiency in cellular networks—a stochastic geometry framework," *IEEE Trans. Wireless Commun.*, vol. 17, no. 4, pp. 2539–2556, Apr. 2018.
- [7] J. Kong, M. Ismail, E. Serpedin, and K. A. Qaraqe, "Energy efficient optimization of base station intensities for hybrid RF/VLC networks," *IEEE Trans. Wireless Commun.*, vol. 18, no. 8, pp. 4171–4183, Aug. 2019.
- [8] O. E. Ochia and A. O. Fapojuwo, "Energy and spectral efficiency analysis for a device-to-device-enabled millimeter-wave OFDMA cellular network," *IEEE Trans. Wireless Commun.*, vol. 67, no. 11, pp. 8097–8111, Nov. 2019.
- [9] R. Tao, W. Liu, X. Chu, and J. Zhang, "An energy saving small cell sleeping mechanism with cell range expansion in heterogeneous networks," *IEEE Trans. Wireless Commun.*, vol. 18, no. 5, pp. 2451–2463, May 2019.
- [10] Y. Su, Z. Gao, X. Du, and M. Guizani, "User-centric base station clustering and resource allocation for cell-edge users in 6G ultra-dense networks," *Future Gener. Comput. Syst.*, vol. 141, pp. 173–185, Apr. 2023.
- [11] G. Zhao, S. Chen, L. Zhao, and L. Hanzo, "Energy-spectral-efficiency analysis and optimization of heterogeneous cellular networks: A large-scale user-behavior perspective," *IEEE Trans. Veh. Technol.*, vol. 67, no. 5, pp. 4098–4112, May 2018.
- [12] F. Baccelli and A. Giovanidis, "A stochastic geometry framework for analyzing pairwise-cooperative cellular networks," *IEEE Trans. Wireless Commun.*, vol. 14, no. 2, pp. 794–808, Feb. 2015.
- [13] Y. Al-Eryani, E. Hossain, and D. I. Kim, "Generalized coordinated multi-point (GCoMP)-enabled NOMA: Outage, capacity, and power allocation," *IEEE Trans. Commun.*, vol. 67, no. 11, pp. 7923–7936, Nov. 2019.
- [14] Y. Li et al., "Air-to-air communications beyond 5G: A novel 3D CoMP transmission scheme," *IEEE Trans. Wireless Commun.*, vol. 19, no. 11, pp. 7324–7338, Nov. 2020.
- [15] M. Elhattab, M.-A. Arfaoui, and C. Assi, "CoMP transmission in downlink NOMA-based heterogeneous cloud radio access networks," *IEEE Trans. Commun.*, vol. 68, no. 12, pp. 7779–7794, Dec. 2020.
- [16] Y. Li, M. Xia, and S. Aissa, "Coordinated multi-point transmission: A Poisson-Delaunay triangulation based approach," *IEEE Trans. Wireless Commun.*, vol. 19, no. 5, pp. 2946–2959, May 2020.
- [17] S. Mukherjee, D. Kim, and J. Lee, "Base station coordination scheme for multi-tier ultra-dense networks," *IEEE Trans. Wireless Commun.*, vol. 20, no. 11, pp. 7317–7332, Nov. 2021.
- [18] G. Zhao, S. Chen, L. Zhao, and L. Hanzo, "Joint energy-spectral-efficiency optimization of CoMP and BS deployment in dense large-scale cellular networks," *IEEE Trans. Wireless Commun.*, vol. 16, no. 7, pp. 4832–4847, Jul. 2017.
- [19] W. Guo, S. Wang, X. Chu, J. Zhang, J. Chen, and H. Song, "Automated small-cell deployment for heterogeneous cellular networks," *IEEE Commun. Mag.*, vol. 51, no. 5, pp. 46–53, May 2013.
- [20] H. S. Jo, Y. J. Sang, P. Xia, and J. G. Andrews, "Heterogeneous cellular networks with flexible cell association: A comprehensive downlink SINR analysis," *IEEE Trans. Wireless Commun.*, vol. 11, no. 10, pp. 3484–3495, Oct. 2012.
- [21] S. Singh, H. S. Dhillon, and J. G. Andrews, "Offloading in heterogeneous networks: Modeling, analysis, and design insights," *IEEE Trans. Wireless Commun.*, vol. 12, no. 5, pp. 2484–2497, May 2013.
- [22] P. Marsch and G. P. Fettweis Eds., *Coordinated Multi-Point in Mobile Communications: From Theory to Practice*. Cambridge, U.K.: Cambridge Univ. Press, 2011.
- [23] I. Hwang, B. Song, and S. S. Soliman, "A holistic view on hyper-dense heterogeneous and small cell networks," *IEEE Commun. Mag.*, vol. 51, no. 6, pp. 20–27, Jun. 2013.
- [24] I. S. Gradshteyn and M. Ryzhik, *Table of Integrals, Series, and Products*, 7th ed. San Diego, CA, USA: Academic, 2007.
- [25] L. F. Williams, "A modification to the half-interval search (binary search) method," in *Proc. 14th Annu. Southeast Regional Conf.*, 1976, pp. 95–101.
- [26] A. Papazafeiropoulos, P. Kourtessis, M. D. Renzo, S. Chatzinotas, and J. M. Senior, "Performance analysis of cell-free massive MIMO systems: A stochastic geometry approach," *IEEE Trans. Veh. Technol.*, vol. 69, no. 4, pp. 3523–3537, Apr. 2020.
- [27] H. He, X. Yu, J. Zhang, S. Song, and K. B. Letaief, "Cell-free massive MIMO for 6G wireless communication networks," *J. Commun. Inf. Netw.*, vol. 6, no. 4, pp. 321–335, Dec. 2021.
- [28] J. Zheng, J. Zhang, J. Cheng, V. C. M. Leung, D. W. K. Ng, and B. Ai, "Asynchronous cell-free massive MIMO with rate-splitting," *IEEE J. Sel. Areas Commun.*, vol. 41, no. 5, pp. 1366–1382, May 2023.
- [29] S. Tombaz, A. Vastberg, and J. Zander, "Energy- and cost-efficient ultra-high-capacity wireless access," *IEEE Wireless Commun.*, vol. 18, no. 5, pp. 18–24, Oct. 2011.
- [30] Y. Zhou et al., "Large-scale spatial distribution identification of base stations in cellular networks," *IEEE Access*, vol. 3, pp. 2987–2999, 2015.
- [31] M. Haenggi and R. K. Ganti, "Interference in large wireless networks," *Found. Trends Netw.*, vol. 3, no. 2, pp. 127–248, 2008.
- [32] J. Ferenc and Z. Nédá, "On the size distribution of Poisson Voronoi cells," *Physica A: Stat. Mechanics Appl.*, vol. 385, no. 2, pp. 518–526, Nov. 2007.